LAPPEENRANTA UNIVERSITY OF TECHONOLOGY
LUT School of Energy Systems
Electrical Engineering

Khaliullin Emil

WIND TURBINE INDIRECT ICE DETECTION AND OPERATIONAL ANALYSIS

Examiners: Professor, D.Sc Olli Pyrhönen
D.Sc Katja Hynynen

ABSTRACT

Lappeenranta University of Technology
LUT School of Energy Systems
Degree Program in Electrical Engineering

Emil Khaliullin

WIND TURBINE INDIRECT ICE DETECTION AND OPERATIONAL ANALYSIS

2016

61 pages, 22 figures, 10 tables and 28 equations

Examiners: Professor, D.Sc Olli Pyrhönen
D.Sc Katja Hynynen

Keywords: wind turbine performance, SCADA, data pre-processing, turbulence, vertical wind shear, air density, indirect ice detection, power curve normalization.

Wind energy is one of the most promising and fast growing sector of energy production. Wind is ecologically friendly and relatively cheap energy resource available for development in practically all corners of the world (where only the wind blows). Today wind power gained broad development in the Scandinavian countries. Three important challenges concerning sustainable development, i.e. energy security, climate change and energy access make a compelling case for large-scale utilization of wind energy. In Finland, according to the climate and energy strategy, accepted in 2008, the total consumption of electricity generated by means of wind farms by 2020, should reach 6 - 7% of total consumption in the country [1].

The main challenges associated with wind energy production are harsh operational conditions that often accompany the turbine operation in the climatic conditions of the north and poor accessibility for maintenance and service. One of the major problems that require a solution is the icing of turbine structures. Icing reduces the performance of wind turbines, which in the conditions of a long cold period, can significantly affect the reliability of power supply. In order to predict and

control power performance, the process of ice accretion has to be carefully tracked. There are two ways to detect icing – directly or indirectly. The first way applies to the special ice detection instruments. The second one is using indirect characteristics of turbine performance. One of such indirect methods for ice detection and power loss estimation has been proposed and used in this paper. The results were compared to the results directly gained from the ice sensors. The data used was measured in Muukko wind farm, southeast Finland during a project 'Wind power in cold climate and complex terrain'. The project was carried out in 9/2013 - 8/2015 with the partners Lappeenranta university of technology, Alstom renovables España S.L., TuuliMuukko, and TuuliSaimaa.

Table of contents

LIST OF SYMBOLS AND ABBREVIATIONS

Symbols

A	[m^2]	Considered area
A_1	[m^2]	Segment area 1
A_2	[m^2]	Segment area 2
A_{exc}	[m^2]	Excluded segment area
A_{sw}	[m^2]	Turbine swept area
C_p		Power factor
crd	[m]	Segment chord length
d		Zero plane displacement
h_{hub}	[m]	Turbine's hub height
h_{Lidar}	[m]	Measuring height of Lidar module
h_1	[m]	Measuring height step of Lidar radar
h_2	[m]	Measuring height half-step
i		Wind speed bin group number
L		Monin-Obukhov stability parameter
M	[kg/mol]	Molar mass of the air
N		Number of measurements taken over the sampling period
N_{WS_i}		Number of power output values belonging to the same wind speed bin
P'	[kW]	Relative power

P_{loss}	[kW]	Total power loss
P_{WS_i}	[kW]	Power output belonging to wind speed bin
$P_{WS_i}^{ref}$	[kW]	Reference power output of wind speed bin
p	[Pa]	Atmospheric pressure
$p^{hub\ h.}$	[Pa]	Atmospheric pressure measured at the hub height
p^{Lidar}	[Pa]	Atmospheric pressure at the measuring level
R	[m]	Turbine rotor radius
$R_{\ dry\ air}$	[J/(kg·K)]	Dry air constant
R_g	[J/(kg·K)]	Universal gas constant
R_s	[J/(kg·K)]	Specific gas constant
$S_{10\ min}$		Sample averaged value
S_{69}	[m^2]	Semisegment area at the height of 69 m
S_{80}	[m^2]	Semisegment area at the height of 80 m
S_{91}	[m^2]	Semisegment area at the height of 91 m
S_{102}	[m^2]	Semisegment area at the height of 102 m
S_{113}	[m^2]	Semisegment area at the height of 113 m
T	[K]	Ambient temperature
$T^{hub\ h.}$	[K]	Ambient temperature at the hub height
T_s	[s]	Sample period
V	[m^3]	Volume
$\overline{WS}$	[m/s]	Mean wind speed

WS_{ref}	[m/s]	Wind speed measured at a reference height
WS_z	[m/s]	Wind speed at the height *z*
$WS_i^{hub\ h.}$	[m/s]	10-minute averaged wind speed value measured at the hub height
$WS_{norm_i}^{hub\ h.}$	[m/s]	Wind speed at the hub height normalized for air density
WS_{TI}^{norm}	[m/s]	Normalized wind speed regarding turbulence component
ws'	[m/s]	Turbulent wind speed
$ws*$		Friction velocity
$Z_{hub\ h.}$	[m]	Turbine hub height
z	[m]	Height
z_{ref}	[m]	Reference height
z_0		Surface roughness
α		Wind shear exponent
κ		Kármán's constant
ρ	[kg/m^3]	Density
ρ_0	[kg/m^3]	Standard air density
ψ		Stability term

Abbreviations

GHG	Greenhouse gas
ISA	International standard atmosphere
LE	Leading edge of the blade
Lidar	Light Detection And Ranging
SCADA	Supervisory Control and Data Acquisition
TI	Turbulence intensity

1 Introduction

According to the World Wind Resource Assessment Report 2014, Europe and Russia along with the USA have a great potential for the wind power. In total it is estimated as nearly 85 TW of energy [2]. The high intensity of the wind in the northern latitudes is both an advantage and limitation of the wind energy sector in the region. On the one hand, energy capacity of the flow imposed to the turbine blades rises with wind speed and air density, which is inversely proportional to the temperature, but on the other hand, these same factors complicate the operation of the turbine. So, strong gusting winds and low temperature promoting an icing of installations impose additional requirements to reliability and durability of the wind turbine design. In avoidance of mechanical overloads of blades at a strong icing or excessively high wind speed, operation of wind turbine, as a rule, is stopped. Thus, monitoring the state of turbines regarding an icing of its structures is an important component of the system reliability.

Special anti-icing mechanisms and ice-detectors are used in construction of the turbines operating in northern climate. However, measurements of these systems may not always be reliable, while the sensor equipment requires additional investments for service and maintenance. One way to reduce costs and improve the reliability of ice monitoring can be the analysis of indirect parameters of turbine operation for the presence of icing. Furthermore, a deeper analysis of the process will allow to assess the effect of icing on the performance of wind turbine.

Aim of the thesis

The aim of this study is the analysis of wind turbines performance in the conditions of cold climate. The effect of weather conditions to the turbine productivity and ice detection methods are briefly discussed. One of the methods is used in analysis of turbine performance and power loss estimation in a case of icing events. The method is not using special detection equipment and allows to detect possible icing by indirect parameters. The results of the analysis are further compared to the information collected directly by ice sensors in order to conclude on applicability of proposed method. The object of study is wind turbine located at Muukko wind farm, southeast Finland.

2 Background

Today the market of wind power is one of the most fast-growing sector of Renewable Energy. The foundation of commercial use of wind farms for receiving the electric power was laid in Denmark at a turn of the 18th century. However, this technology took broad development during the period since eightieth years of the 20th century when commercial projects gained profitable character. By the beginning of 2015 the total installed capacity of wind power has amounted 432.88 gigawatts [3]. The development of wind energy bears great potential that can lead to large changes in the market. Nevertheless, from the very beginning this process is subjected of both driving and limiting factors. At the same time the development of wind energy in cold climate zones have their own specifics.

2.1 Key drivers of wind energy development

Three important challenges concerning sustainable development, i.e. energy security, climate change and energy access make a compelling case for large-scale utilization of wind energy.

Energy security

The rapid growth of the economy, and hence, of the energy consumption exacerbates the issue of energy insecurity and uncertainty in countries that depend on energy and energy resources export. Europe's import dependency on fossil fuels is expected to rise and imported gas is likely to make up to 80% of consumption by 2030 [2]. Wind generators during operation does not consume fossil fuel. Operation of the wind generator with a power of 1 MW in 20 years, by approximate estimates, allows to save about 29 thousand tons of coal or 92 thousand barrels of oil, and as a result the total savings can amount to millions of dollars.

Ecology

According to the information of The Intergovernmental Panel of Climate Change (IPCC) between 1971 and 2010, global emissions of CO_2 have increased by almost 2 times, where slightly less than a half of the emissions is the share of electricity sector. In the production of electricity by wind mill plant, CO_2 emissions are absent. The 1 MW wind turbine reduces annual emissions of 1,800 tons of CO_2, 9 tons of SO_2, 4 tons of nitrogen oxides. Thus, the development of this sector is seen as an invaluable contribution to struggle against the greenhouse effect. The need to reduce GHG emissions is yet another major driver for countries to set up wind power plants [4].

Energy access

In some areas with low population density and weak road infrastructure and transportation communications wind power is of particular relevance. This eliminates the necessity of building a centralized power supply, which is not always cost-effective, and also solves the problem of delivery of fuel for power plant. This advantage may be particularly relevant in some northern areas and localities.

High energy content

The energy that carries the wind flow is directly dependent on its density, which rises with contrary to the air temperature. In this way, Nordic countries have the further advantage of wind power development.

2.2 Main challenges of wind power in cold climate

Low temperature

In northern latitudes, the ambient temperature can continuously fall to the extreme negative values. In such circumstances, many structural materials used in the construction of turbines can substantially change their properties. For instance, steel, while the cold become more brittle, and composite materials may get microcracks due to uneven shrinkage. Also, significantly increases the viscosity of the lubricant, which may affect the operation of the turbine rotating mechanisms.

After a long break in the cold conditions, winding of the generator or transformer may be subject to thermal shock during start-up at low temperatures, rubber lose fluidity, which can affect the sealing of the installation parts. [5]

Snow

Loose snow structure allows it to penetrate into the housings of the turbine, as well as block the ventilation dots. All that threatens the accumulation of moisture inside of housing, as well as the deterioration of the heat sink of the installation.

Icing

Icing of turbine structures is the most crucial limitation for wind turbines application at northern altitudes. Ice accretion complicates turbine operation and affects its performance by [5]

- Changing blades profile;
- Hindering rotation of movable joints of the turbine;
- Increasing static load to the rotor and turbine joints;
- Distorting the dynamic balance of the rotor and accelerating fatigue;
- Hindering the access to the nacelle for maintenance personal;
- Threat with hit of the flown-away ice chunks.

The problem of icing and the process of ice accretion is discussed in more detail in the following chapter.

3 Icing

3.1 Phases of icing

Icing should be understood as accumulation of ice or snow mass on turbine structures, which is negatively affecting its operation. Ice formation process can be considered as a cycle of certain phases.

Phases of icing propagation

Generally, ice formation process in turbine structures can be divided into two parts - active and passive. The active part is represented by time interval, where weather conditions are favorable for ice formation and ice is actively formed on a turbine surface, whereas the passive part is a time when ice remains on the surfaces but is not forming any longer.

According to [6] the following phases can be distinguished:

- Meteorological icing;
  Period of time when the meteorological conditions for ice accretion are favorable.
- Instrumental icing;
  Period of time when the ice is attached to wind turbine structures.
- Incubation time;
  Time delay between meteorological and instrumental icing phases.
- Recovery time;
  Time when ice remains steady on the wind turbine surface or melting.

The abovementioned phases of icing propagation are interpreted in Fig. 3.1

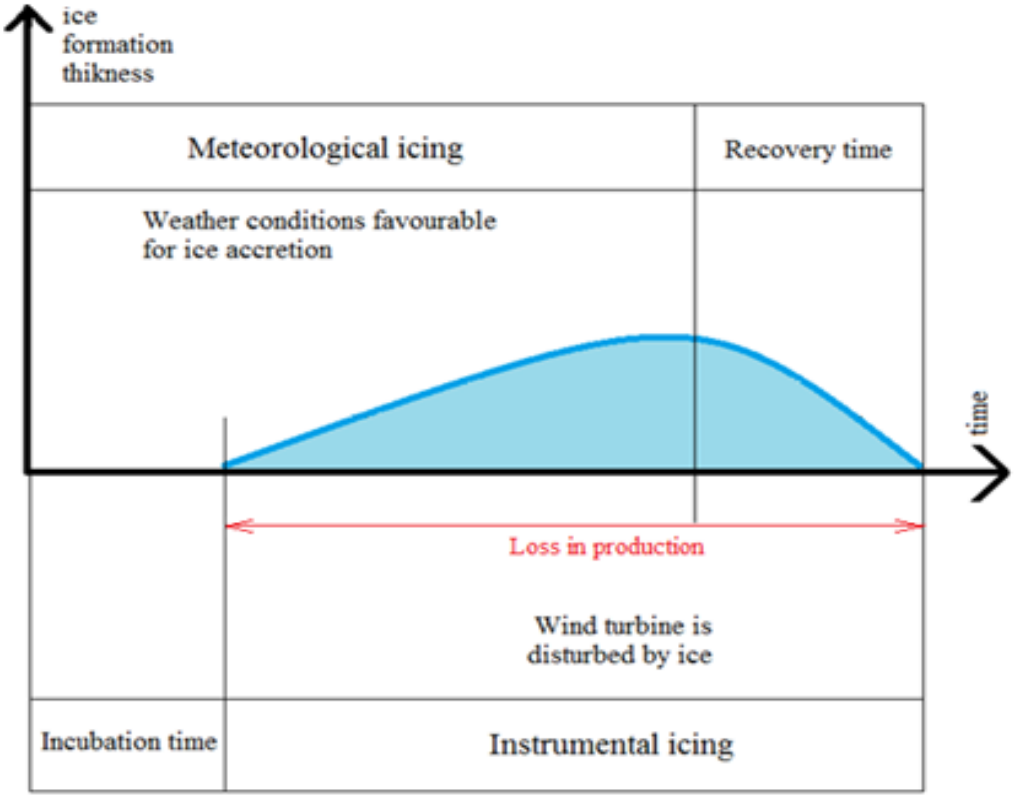

Fig. 3.1 Phases of icing propagation

The period of instrumental icing is also a time when the turbine production is affected by ice. Various heating systems of wind turbine blades and anti-ice plating are applied in modern wind turbines in order to reduce this period. However, the time of icing along with the rate of ice accretion are directly dependent only on the atmospheric conditions, in which the electrical installation is operating.

Atmospheric conditions causing ice Technically speaking, for the process of ice accretion, it is necessary and sufficient that the following two conditions are met:

- Temperature of the turbine surface is equal or lower than crystallization temperature of the water accumulated in the surrounding atmosphere concentrating on the surface;
- Sufficient amount of this water in this atmosphere.

Thus, such parameters as ambient temperature, humidity and wind speed determine icing process formation. Depending on a combination of these parameters, various forms of icing differing on structure, density and adhesion properties are possible.

3.2 Ice types

By nature of formation, ice accretion can be divided on precipitation icing and in-cloud icing. In the first case the source of moisture is precipitation in the form of rain or snow, whereas in the second – it is cloud or fog droplets. [6]

Precipitation icing group is presented by glaze and wet snow icing.

Glaze is a solid-ice layered formation in a way similar in appearance with sugar glaze. Wet snow is a partly-melted snow flakes, forming clusters that have a porous loose structure. The examples of such formations can be seen at everyday life. Glaze is similar to winter patterns on the window. Wet snow is often seen covering the tree branches after a snowfall when the temperature is close to zero.

The group of in-cloud icing is presented by glaze, hard rime and soft rime.

Hard and soft rime is a formation mainly concentrated on the leading edge of turbine blades similar to that one, which appears on the wings of aircraft at contact with the cold running stream. The examples are shown in Fig. 3.2 [7] and Fig. 3.3 [8].

Fig. 3.2 Ice accumulation on the leading edge of wing. [6]

Fig 3.3 Ice accumulation on the leading edge of wind turbine. [8] Photo credit: Kent Larsson, ABvee, Sweden.

Icing type and its characteristics vary depending on the weather conditions.

Ice type classification and its characteristics, formation parameters, typical duration of icing period and moisture sources are given in Table 3.1 [9]. Rime ice and glaze formation dependence on temperature and wind flow speed is presented in Fig. 3.4 [10].

Table 3.1 Ice type classification and its characteristics

Atmospheric ice type classification				
Nature of formation				
Precipitation icing		In-cloud icing		
Glaze (drizzle)	Wet snow	Glaze	Hard rime	Soft rime
Water source				
Freezing rain, Freezing drizzle	Partly melted snow crystals with high water content	Wet in-cloud icing	Super cooled liquid water droplets from clouds or fog	
Ambient temperature, ° C				
-10 – 0	0 – +3	-6 – 0	-20 – 0	-20 – 0
Water content in air				
Medium	Very high	High	Medium	Low

Wind speed, m/s				
Any	Any	See Fig. 3.4	See Fig.3.4	Fig3.4
Typical duration of ice event				
Hours	Hours	Hours	Days	Days

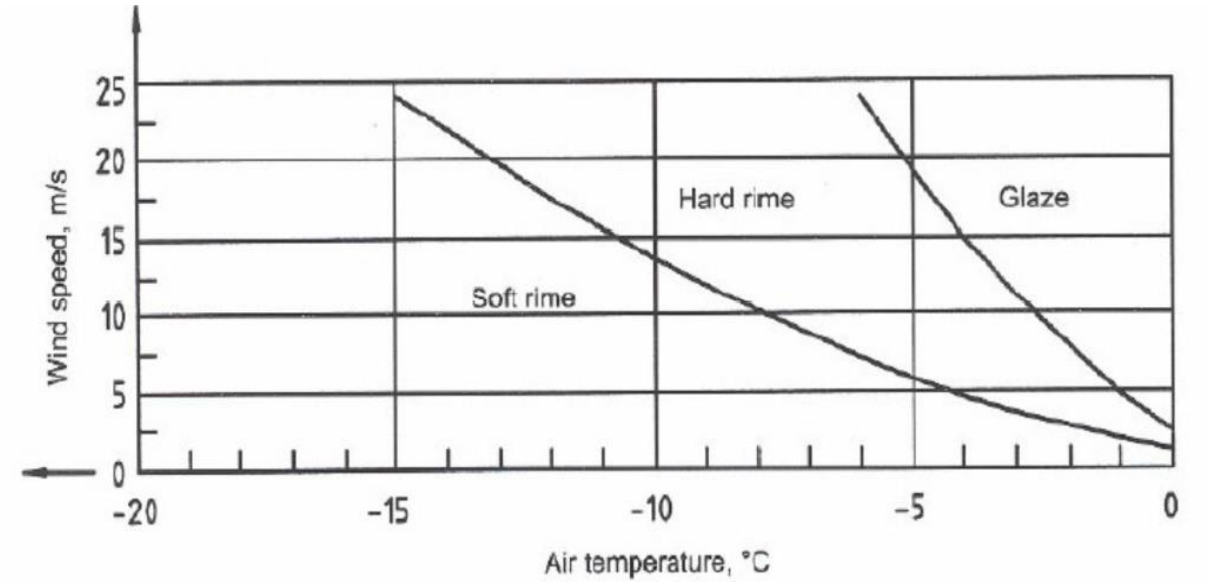

Fig. 3.4 Ice rime and glaze formation dependence of air temperature and wind speed. [10]

Here should be noted that wind promotes accretion of ice on a surface, increasing the rate of heat exchange between the body of the turbine and the environment (reducing incubation time) and transferring water droplets from atmosphere towards turbine side. At the same time strong wind - on opposite - can effect removal of the ice or hinder its adhesion.

According to the World Weather and Climate information source in the location of the wind farm the average minimal temperature stays below 0 from October up to April and therefore, ice formation processes with varying degree of probability can be expected for more than six months. Average, minimum and maximum temperature in Lappeenranta (near Muukko wind farm location) are given in Table 3.2. [11]

Table 3.2 Average, minimum and maximum temperature at Lappeenranta

	Temperature		
Months	**Normal**	**Warmest**	**Coldest**
January	-7.4°C	-4.4°C	-10.8°C
February	-7.7°C	-4.4°C	-11.4°C
March	-3.1°C	0.5°C	-6.9°C
April	2.5°C	7.0°C	-1.8°C
May	9.9°C	15.6°C	4.0°C
June	14.8°C	20.2°C	9.3°C
July	16.9°C	22.1°C	11.7°C
August	14.9°C	19.7°C	10.4°C
September	9.3°C	13.4°C	5.6°C
October	4.1°C	7.0°C	1.4°C
November	-1.1°C	1.2°C	-3.7°C
December	-5.2°C	-2.4°C	-8.4°C

It should be noted that the data shown in Table 3.2 represents temperature at the ground level. It is necessary to take into account the change of temperature with altitude.

3.3 Ice accretion problem

Ice accretion may considerably increase the mechanical load to the wind turbine rotor and structures that enhances imbalance and fatigue of turbine constructions that in turn, can significantly reduce lifetime of the system.

The iced wind turbine design also represents a threat to security for the people in the immediate vicinity of installations as breakaway ice pieces can scatter at rather long distance. Presently, there are not so many cases of injury known or documented although some researches has been done on modeling a situation of ice throw. For instance, in accordance to [12] a dynamic modulation has shown that a 1 kg plate-like fragment of ice could travel up to 350 m from the base of the turbine.

One more considerable problem caused by ice is distortion of an aerodynamic profile of the turbine blades that leads to reduction of the wind flow up-lifting force and consequently, increases energy loss.

The effect of icing at leading edge (LE) of the turbine blades on rotor power is illustrated in Fig. 3.5 [10].

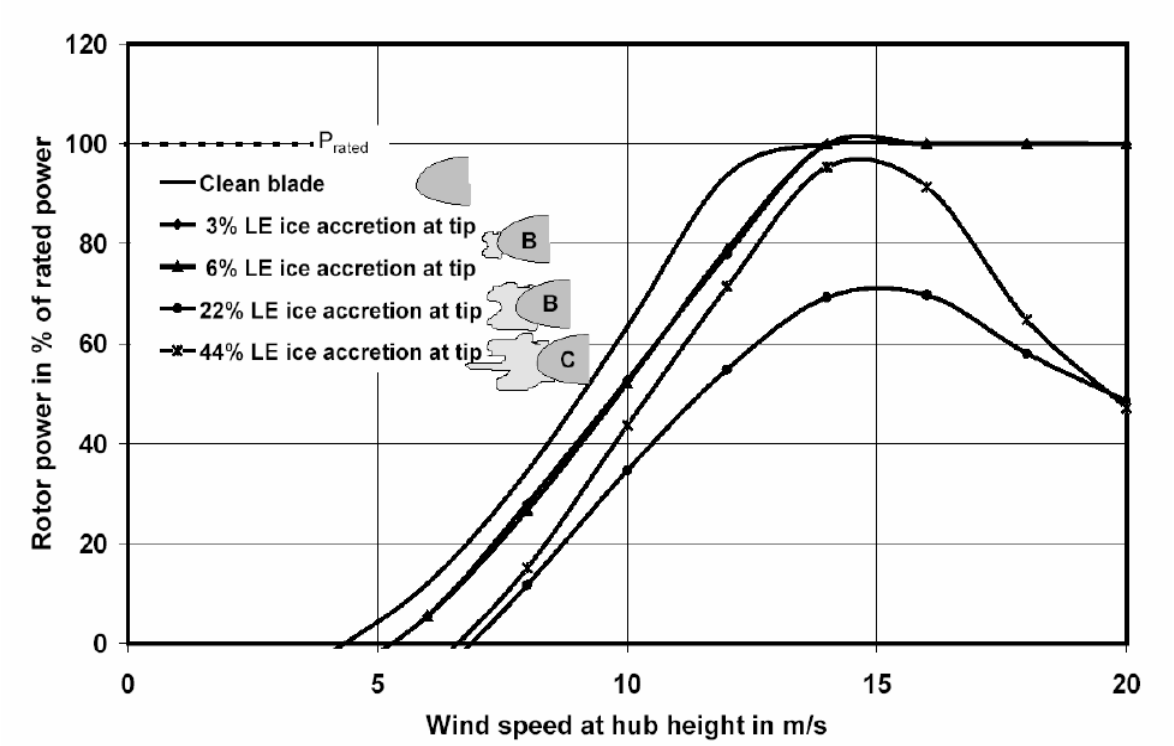

Fig. 3.5 Calculated power curve for a pitch controlled fictitious turbine with different types of ice accretion. [9]

From Fig, 3.5 it is clearly seen that the icing has a significant effect on turbine efficiency even at low values of ice accretion. This drawback, in contrast to the others has instantaneous effect on the system performance.

These problems are the reasons for which the prediction, monitoring and control of icing process is an important aspect of trouble-free and reliable operation for wind turbines. Many ice detection tools have been designed recently to help to estimate power loss and avoid unexpected brakes in wind power production.

3.4 Ice detection

There are a number of ice detection systems designed to gain information on wind turbine performance during the periods of possible icing. The main element of such systems is the ice sensor, operational principle of which is based on one or another property change tracking used to detect the presence of ice by direct or indirect signs accompanying its appearance. For instance, such a sign can be a change of reflection properties, conductivity or thermal variation caused by ice accretion on measuring surface.

Method systematization indicating the ice effect on property used as the icing indicator along with the way of sensor positioning on the turbine are given in Table 3.3. [10] [13]

Table 3.3 Direct ice detection methods

Method	Ice effect on the tracked parameter	Mounting position	
		nacelle	blade
Direct ice sensing methods			
Ultra-sonic /micro wave	Emitted wave energy attenuation	●	
Resonant frequency	Resonator frequency reduction	●	
Vibrating diagram measurement	Damping of vibration		●
Electrical properties of sensing path	Deviation from the nominal value of the resistance, inductance or capacitance		●
Ambient temperature	Delays sensor response on temperature changes		●
Optical scanning	Change in light bin energy	●	
Stereo imaging	Image spectral change	•	-

In some methods ice accretion monitoring is done by measuring of parameters that may signalize icing indirectly. Absence of necessity for additional measuring equipment is the main advantage of such systems, enabling them to build an auxiliary channel for ice accretion monitoring.

Some of these methods with description are listed in Table 3.4. [9] [10] [13]

Table 3.4 Indirect ice detection methods.

Method	Analysis principle	Ice effect on the tracked parameter	Mounting position	
			nacelle	blade
Expected - real power difference	Calculated by means of aerodynamic modelling output power level is compared to the actual output. A significant difference in the calculations and indications can be caused by ice accretion	Positive power difference	-	
Anemometer reading difference	The reason for differing readings of the heated and unheated anemometer may be ice accretion on the last one.	Hinder iced anemometer rotation	●	
Dew point	At a certain coincidence of temperature and humidity (dew point) icing is most probable	-	●	
Blade resonant frequency	The resonant frequency of turbine blade changes for the ice accretion as its mass grows	Damps nominal resonant frequency		●
Cloud height measurement	The probability of icing of the blades is greatly increased if the clouds are located at their level	-	On the ground level	
Noise measurement	Rotation of iced blades, as a rule, is followed by higher level of the producing noise	Noise profile distortion	On the ground level	

All the above methods allow to detect ice accretion with some accuracy and have its advantages and disadvantages.

Disadvantages include:

- Impossibility of installing the ice-sensitive element directly on the surface of the blades;
  Problem is that in such systems the measuring height does not correspond to the actual maximum height of the blades. In this way, in the systems where ice sensors are located on the turbine nacelle the measurement is carried out at 50-70 meters lower than the actual location of the blades what can negatively affect the accuracy of ice tracking.

- Inability to detect ice formation within a scatter area using only one sensor;
  In such systems the measurements are collected only from a single point where the sensor is mounted.

- Inability to install ice detection system on existing wind turbines;
  Some of these ice detection systems cannot be easily mounted on operating turbines.

- Not weather-indifferent measuring;
  Ambient parameters have a great impact on detection accuracy.

Complexity of measuring equipment and the need for additional maintenance and control.

These drawbacks affect measurement accuracy and reliability of the ice detection. At the same time, implementation of multiple ice detection systems could increase reading reliability of sensors but it negatively affects the cost and complicates measuring system. However, indirect methods that do not require additional equipment, can serve as a primary detection system or can be used as an auxiliary source of information. One of such indirect ice detection methods based on SCADA and Lidar measurements will be discussed in the next chapter.

4 Proposed method of indirect ice detection

Proposed method of indirect ice indication is based on data provided by The Supervisory Control and Data Acquisition System (SCADA) and Lidar. The SCADA system is a wind turbine built-in system. Lidar module is located at Muukko wind farm (Lappeenranta, southeast Finland).

The object of study is an Alstom wind turbine ECO 110:

- rated power - 3 MW;
- rotor diameter – 110 m;
- number of blades – 3;
- tower height (hub height) – 90 m.

The winter from November 2014 to April 2015 is taken for analysis. According to [11] during this months the weather remains favorable for ice formation.

4.1 Power plant placement description

The choice of placement of wind farms is based on consideration to maximize electrical efficiency, which in turn is dictated by the nature of the wind flows distribution. So, wind flows distribution explains the tendency to select the location of plant in a coastal flat zone – in-shore and off-shore. The Muukko wind farm is located near a lake.

Besides, hostile environment with quickly changing weather, low inaccessibility for service, as a rule are the main distinctive features of wind turbines operation. So, the location of the wind farm may affect much the operation stability of the system.

For a description of the icing characteristics of the location of The Muukko wind farm, Finnish Wind and Icing Atlases are used [14]. The picture of a passive and active icing conditions within winter month (January) is obtained and presented below (Fig. 4.1 and Fig. 4.2). At the map Muukko power plant is found near Lappeenranta city. The approximate location is additionally marked with wye marker.

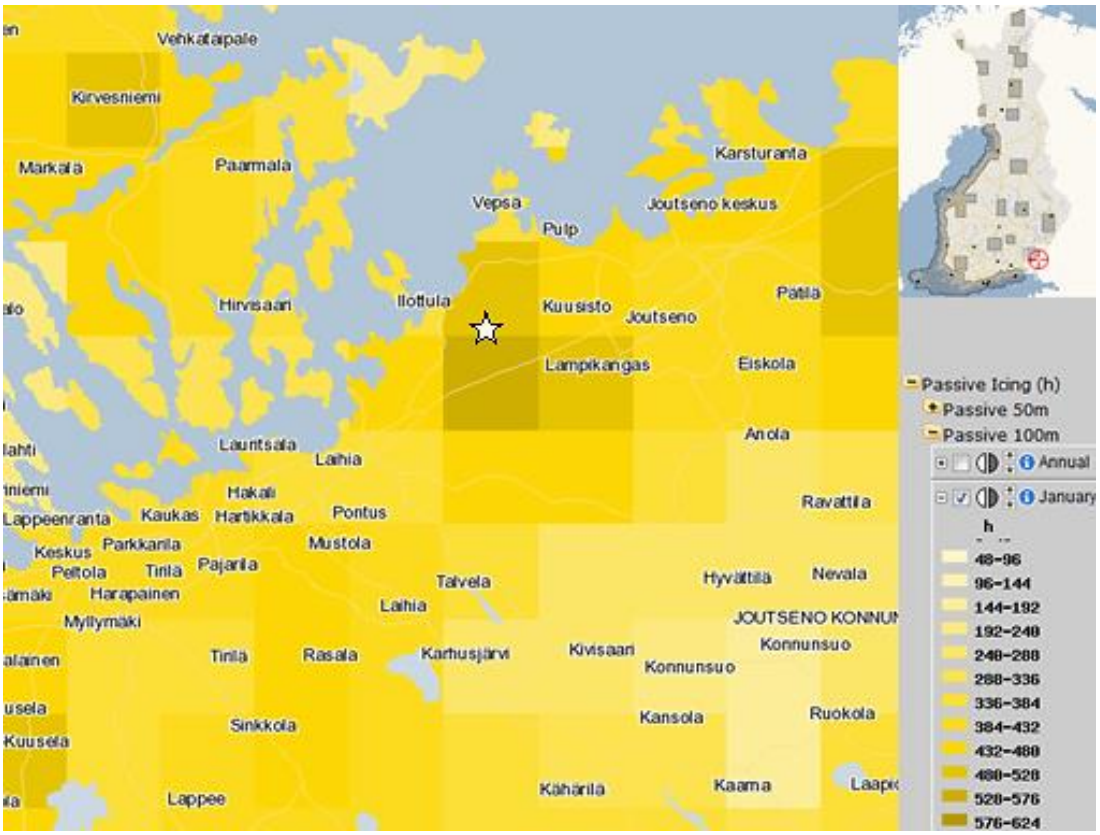

Fig. 4.1 Passive Icing, Jan, 100m [14]

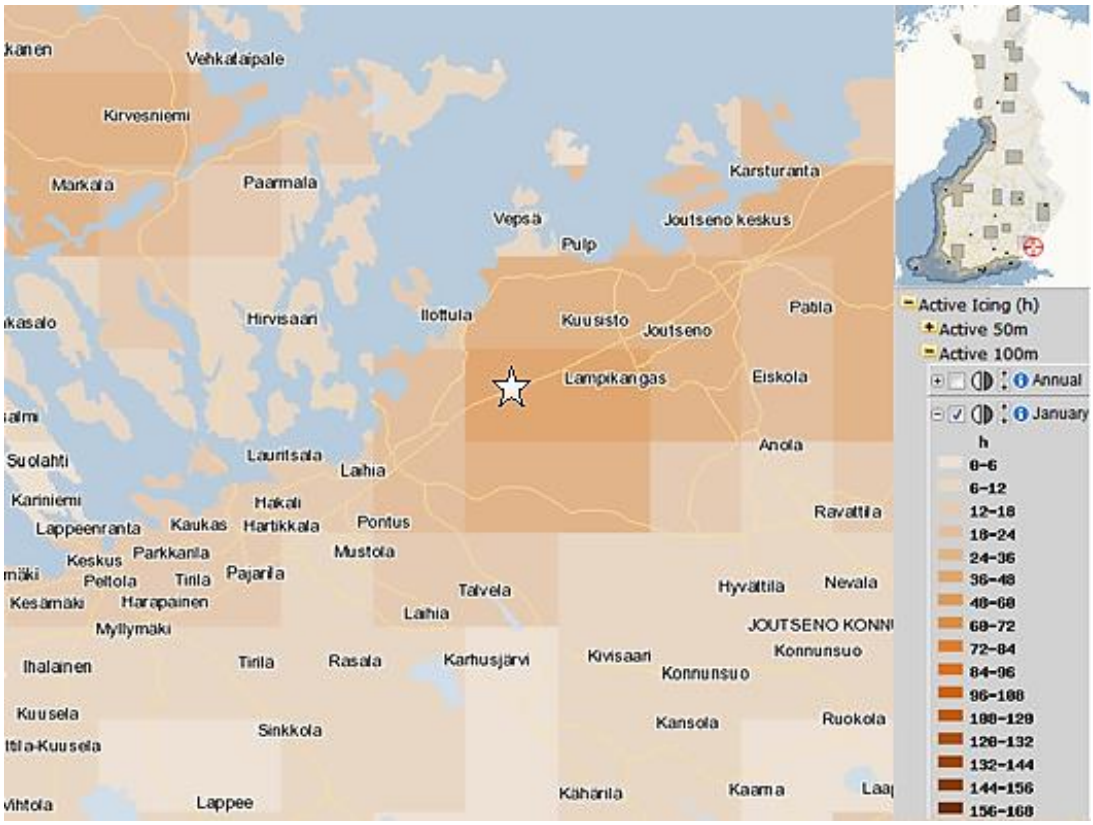

Fig. 4.2 Active Icing, Jan, 100m [14]

Active icing conditions in the area favorable for turbine operation and on average do not exceed 36 hours (5%) in the coldest winter month, which corresponds to relatively low probability of drastic failure or blockage time due to construction icing. However, passive icing indicator for January is quite high –336-384 h what is about a half of the period duration.

In addition, annual wind speed intensity map is presented in Fig. 4.3.

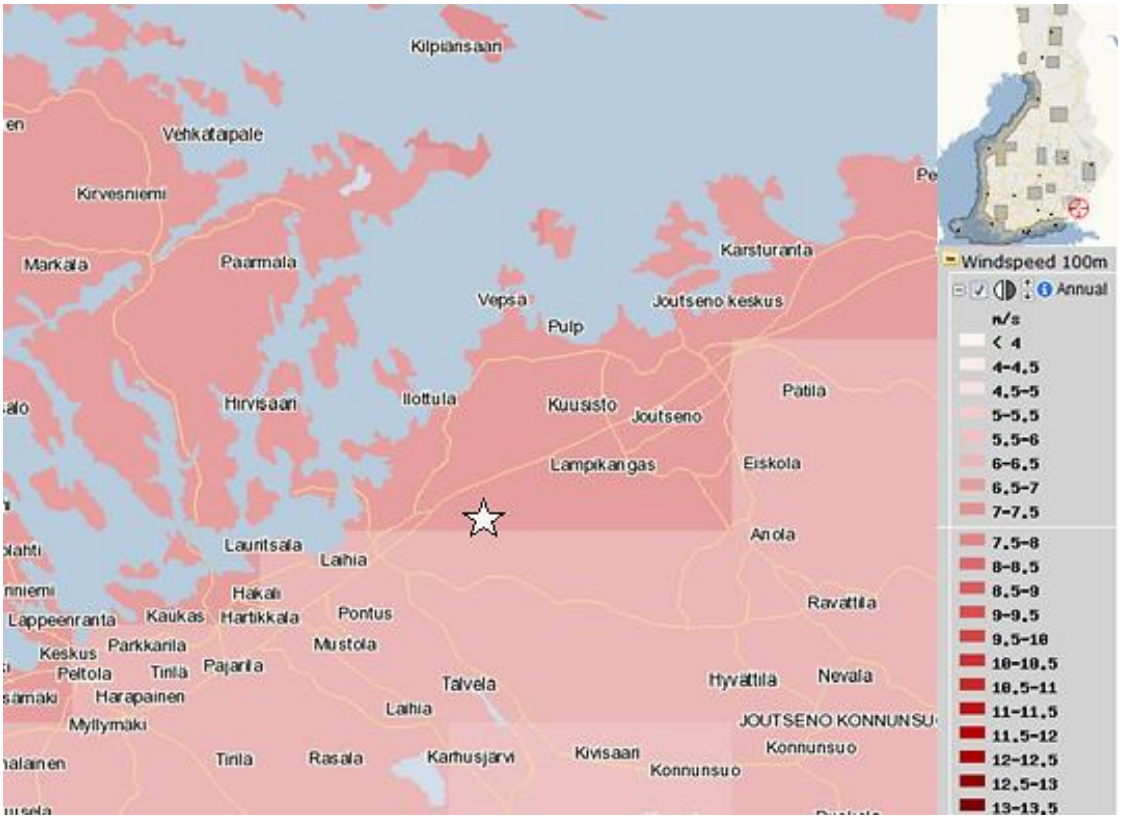

Fig. 4.3 Annual Wind Speed, 100m [14]

Wind conditions of the place are favorable for power production. The average wind speed fluctuates around 6.5 – 7 m/s, which is much higher than the cut-in speed of the turbine, and much lower than the maximum operational speed (cut-down speed).

4.2 Method description

Under natural conditions, the process of icing is not instantaneous. As mentioned in subsection 3.1, the process is inert and has its incubation and recovery time. As a rule, duration of instrumental icing is measured by hours or days and depends on the weather conditions, which are also rarely changed abruptly. In this way, the impact, followed by icing, has to have a long-term nature. This assumption forms the basis of the analysis idea, in which the effect of wind turbine efficiency reduction should be consecutive and steady. In a case of long-term declination of turbine efficiency, operating in ice storm conditions, it can be concluded on the possible presence of ice on the turbine structures. Thus, the level of power loss can be approximately estimated.

In order to determine the degradation in turbine performance, it is proposed to compare the current value of power output with a reference value. Reference value is calculated as an arithmetic mean of all values for output power during the turbine operation in a certain intervals of wind speed. The wind speed bins are taken from 4 m/s (cut-in speed) and further up with the increment of 0.5 m/s.

$$P_{WS_i}^{ref} = \frac{\sum P_{WS_i}}{N_{WS_i}} \tag{4.1}$$

where

$P_{WS_i}^{ref}$ – reference power output of wind speed bin *i*;

P_{WS_i} – power output belonging to wind speed bin *i*;

N_{WS_i} – the number of power output values belonging to the same wind speed bin;

i – wind speed bin group number.

However, as the measurements of wind speed are taken in volatile conditions and some tracking parameters are weather-dependent the data is yet to be adopted in order to provide equality of comparison.

The steps taken in the analysis are discussed further.

4.3 Data sources

4.3.1 The Supervisory Control and Data Acquisition system

The main advantage of the system is that wind turbine health and performance is always traced. It allows to increase reliability of power supply and in due time to react to the failures. Input information for monitoring and analyzing of the wind turbine operation is an array of data transmitted by SCADA system. The system allows remotely to obtain sets of different measured parameters - taken by sensors mounted directly to the turbine – averaged through a given period of time. A sample time step is selected from a minute's range, for example, one data file in 10 minutes. It helps to reduce data storage and transmission costs and amount of required equipment. However, in this way the accuracy of monitoring suffers but not to the crucial point.

In addition, the system is capable to solve certain supervisory control tasks by means of starting, stopping or resetting the turbine in case of small operational errors, what is especially actual for the wind farms, which locate far from roads and towns. For these advantages SCADA records is a major data source for monitoring wind turbines condition in the last years [15].

SCADA data itself is a set of time series data which yet have to be analyzed at the following stage. In particular, it is possible to estimate dynamics of parameters of a single turbine operation regarding its stable power generation. By passing the data through the analytical apparatus it is possible to recreate the picture of wind turbine performance.

Data collected for ongoing analysis include:

- generator rotational speed, and
- generator active power.

4.3.2 Lidar

Atmospheric Lidar radars are widely used to monitor meteorological variables. LIDAR is a measuring system that utilizes a laser beam as a measuring tool. This system allows to carry out various types of measurements in the range of heights up to hundreds of meters. A simplified block diagram and operational principle are represented in Fig. 4.4

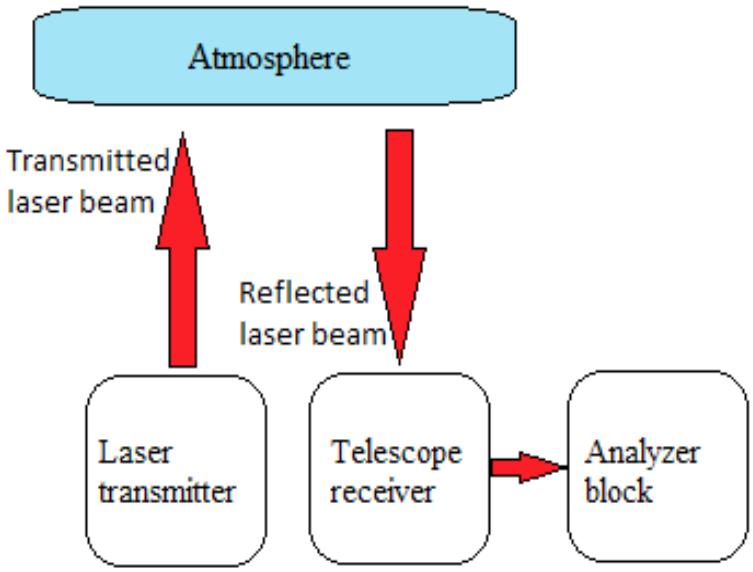

Fig. 4.4 Lidar operational block diagram

The system consists of two main elements – laser and telescope. The laser beam emitted towards the object of interest is adjusted in compliance (by frequency, energy etc.) with measurement characteristics of the recipient. The telescope carries out a function of the beam receiver reflected by object. Changes undergone by a beam after reflection are a subject of the analysis carried out in analyzer block.

So, at various configuration of a beam it is possible to take selective measurements of concrete characteristics of the studied object.

- Data directly or indirectly collected for ongoing analysis include information on: Wind speed and direction at the heights of 47, 69, 80, 91, 102, 113 meters;
- Turbulence intensity;
- Wind shear;
- Ambient temperature;
- Ambient pressure;
- Ambient humidity.

4.3.3 Other sensors used

Method performance and operability of the indirect detection is determined by comparing the analysis results with the data obtained directly from the ice sensors. The research turbine is equipped with 2 different nacelle-mounted ice detectors, hereinafter referred to as sensor A and sensor B.

Sensor A ice detection mechanism is based on change of resonant frequency of vibrating probe. The resonant frequency changes with mass of the probe, which increases in a case of ice plating. In such a way, these changes signalize icing event.

Operation principle of the Sensor B is based on ultrasonic waves damping. At appearance of ice, the passage of the ultrasonic wave is hindered and the difference between emitted and received wave's energies rises, and thus, attenuation is taken as a signal of possible icing event.

4.3.4 Camera

Web camera (2.0-megapixel Day/Night 20x HD PTZ Pendant Dome Camera) is mounted on the nacelle of the turbine and positioned so that it monitors the two thirds length of the turbine blade taking a picture every time the blade passes by.

During the work with images, the following weaknesses of the system have been revealed:

- Camera is mounted far from the blade;
  Thus, to identify glaze or other thin ice formation is problematic.
- Poor visibility during dark, fog and heavy precipitation
  The camera is equipped with infrared light. However, night time lights of turbine disturb its operation.
- Poor contrast;
  The blades have white color that hinder ice and snow detection.
- Camera with motion detector does not take pictures when turbine is standing;
  However, ice accretion process can be in progress during all the time. Thus, the pictures are mainly available for daytime and only when turbine blades are in rotation.

An example of the picture showing rime ice accretion at the leading edge of the blade is presented in Fig. 4.5.

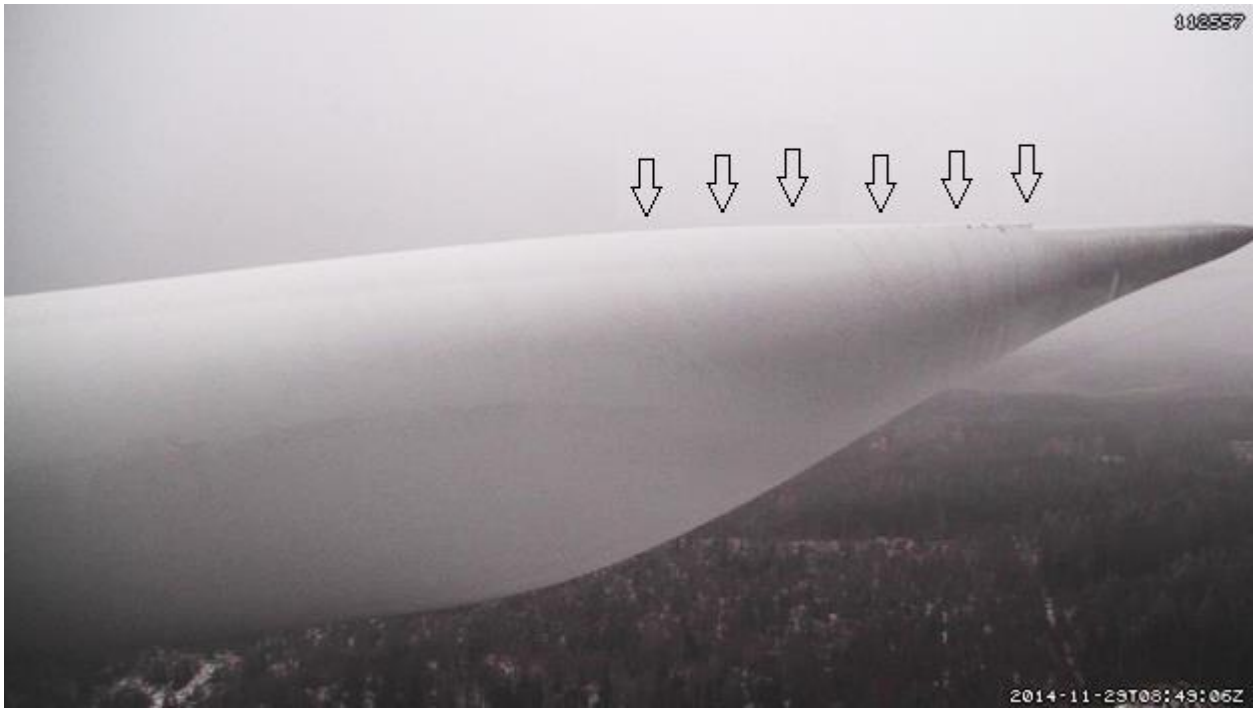

Fig. 4.5 Ice accretion at the leading edge of the blade

Ice accumulation is observed along the edge of the blade (indicated by the arrows) except for the tip region, where it is dropped down.

Pictures are used additionally for validity of indirect detection applied in further analysis.

4.4 Data preprocessing

Data adaptation process includes two steps: filtration and normalization. Wind speeds were normalized and corrected according to the IEC 61400-12-1 standard.

4.4.1 Filtration

At this step the data have to be filtered out for the cases with high measurement uncertainty. Despite of the fact that at this step the volume of data is reduced, the use of filters is of great importance as the analyzed SCADA and Lidar data sets consist of averaged values and in this regard, already bear an inaccuracy share.

Filters taken for preparation of the data and the rationale for its application are described below.

Wind data availability filter

First, the data is filtered for wind data availability.

In order to reduce the amount of handling information Lidar system averages all the wind data measurements so that every transmitted sample value represents a number calculated as:

$$S_{10\,min} = \frac{\sum_1^N s_i}{N} \tag{4.2}$$

where $S_{10\,min}$ is a sample averaged value, s_i is an instant measured value, N is a number of measurements taken over the sampling period. Sometimes, for different reasons the number of measurements taken by the system is lower than the set value N. In such cases the reliability of measuring suffers. To indicate such cases, the system calculates the number of valid measurements taken in the sample for every parameter. This number is expressed in per cents from the set number N and called availability. In our calculations we set the availability factor higher or equal to 60% that allows to discard the cases with relatively impure sample rate.

Wind direction filter

The next filter applied is wind direction filter. Wind speed and direction are measured by Lidar. However, in some case when the wind comes from a certain directional range (blocked sector) the passage of the flow can be hindered by the presence of neighboring turbines. The two nearby turbines, the research turbine A1 and also A2 are influencing in the flow when the wind direction

is from the direction of the turbine to the Lidar. The radius of disturbance is relatively large, the effect of which is even stronger than for met mast, because the Lidar beam is not directly upwards from the device. It can distort the measurement readings. To avoid this effect, the measurements taken when the wind comes from the blocked sector (from 348 to 183 degrees) were excluded from the analysis.

Generator shaft speed filter

Generally, from the ten-minute range perspective, wind flow rate is a parameter of a high volatility. This is especially pronounced at the presence of gusty winds. So, wind turbine operation is usually accompanied by frequent stops and starts due to the low inertia of the mechanism. At the time of acceleration and deceleration the turbine power generation process has not stable character. In order to mitigate the impact of these transient processes, the processing data has been filtered for minimal generator rotational speed - higher or equal 1000 rpm. This filter allows to exclude the cases where the low inappropriate level of power output is largely explained for the work of the turbine on the acceleration or deceleration.

4.4.2 Data normalization

The need for data normalization is mainly dictated by the necessity to take into account the relation of the analyzed airflow parameters on height above the ground.

Steps taken for data normalization and the rationale for its application are described below.

Air density: temperature, humidity and pressure

The amount of kinetic energy imparted to the wind turbine at a collision of the air molecules and the blades will depend on both the flow rate and on the number of molecules per unit of volume in the flow. So, the energy intensity of the air flow induced to the turbine is proportional to its density. Standard air density ρ_0 is equal to 1.225 kg/m^3 (under conditions of standard temperature of 15°C and standard pressure of 1 atm).

The ideal gas low binds all these parameters in a single equation:

$$pV = \frac{m}{M} R_g T \tag{4.3}$$

where

p [Pa] – atmospheric pressure;

V [m^3] – volume;

M [kg/mol] – molar mass of the air;

T [K] – ambient temperature;

R_g [J/mol·K] – universal gas constant.

Dividing both parts of equation (4.3) by volume and considering that the density ρ is a mass per unit volume we obtain the equation for density dependence on pressure and temperature:

$$\rho = \frac{p \cdot M}{T \cdot R_g} \tag{4.4}$$

A specific gas constant R_s can be derived from R_g:

$$R_g = M \cdot R_s \tag{4.5}$$

The dry air constant, $R_{dry\ air}$ is equal to 287.058 J/(kg·K) and then the equation (4.4) can be rewritten with a specific gas constant for dry air:

$$\rho_{dry\ air} = \frac{p}{T \cdot R_{dry\ air}} \tag{4.6}$$

Knowing temperature and pressure at the certain height, it is possible to determine the corresponding air density. According to (4.6), air density at the height of 91 m (turbine hub height) can be calculated as:

$$\rho_{air}^{hub\ h.} = \frac{p^{hub\ h.}}{T^{hub\ h.} \cdot R_{dry\ air}} \tag{4.7}$$

where

$p^{hub\ h.}$[Pa] – atmospheric pressure measured at the hub height;

$T^{hub\ h.}$ [K] – ambient temperature at the hub height.

Atmospheric pressure and temperature measured at the ground level differ from the actual values at the hub height as these parameters are height-dependent.

Atmospheric pressure falls with height due to two reasons: the decrease in the mass of atmospheric column above the point of observation and decrease in the density of the atmosphere gases as at height atmosphere becomes more rarefied. However, the reduction of air density with height matters if to consider all atmosphere making about 10000 km of height. In fact, the lower layer of the atmosphere — the troposphere — contains 80% of mass of air gases, where its density changes insignificant. Thus in the considered altitudes (hub height) the air density can be taken as constant. In this way, the height above the ground level is the only factor effecting pressure change.

Atmospheric pressure change can be described as vertical fluid pressure variation which is found as:

$$\Delta p = -\rho \cdot g \cdot \Delta h \tag{4.8}$$

where g goes for acceleration of gravity and delta symbol indicates the change in a given variables of pressure and height. In such a way, atmospheric pressure at hub height $p^{hub\ h.}$ can be found as:

$$p^{hub\ h.} = p^{Lidar} - \rho \cdot g(h_{hub} - h_{Lidar}) \tag{4.9}$$

where $p^{Lidar}$is atmospheric pressure at the measuring level, h_{hub} is a hub height, h_{Lidar} - measuring height of Lidar module.

Ambient temperature T^{Lidar} is measured by Lidar module and corrected according to the height by environmental lapse rate.

The environmental lapse rate is the rate of decrease of temperature with altitude in the stationary atmosphere at a given time and location. On average, an international standard atmosphere (ISA) is defined with a temperature lapse rate of 6.49 °C /km (1.98 °C/1,000 ft).[16]By this token the appropriate temperature at the hub height is found as:

$$T^{hub\ h.} = T^{Lidar} - 0.0065 \cdot (h_{hub} - h_{Lidar}) \tag{4.10}$$

So, wind speed at the hub height normalized for air density will be found as:

$$WS_{norm_i}^{hub\ h.} = WS_i^{hub\ h.} \cdot (\frac{\rho_{air}^{hub\ h.}}{\rho_0})^{\frac{1}{3}} \tag{4.11}$$

where $WS_i^{hub\ h.}$ [m/s] – 10-minute averaged wind speed value measured at the hub height.

Turbulence Intensity

Turbulence is random continuously changing fluctuations in wind flow differing in speed and direction from the main vector of propagation, and superimposed on the mean value of the wind. When the airflow passes over the ground, turbulence can be caused by surface roughness and topographical features, vertical wind shear, and the presence of convection stirring in troposphere layers.

The turbulent component of the flow bears in itself an additional energy. This energy influence turbine performance assessment. As it was mentioned earlier [17] turbulence accounting brings its changes to the power curve form. The effect on power curve is illustrated in Fig. 4.6.

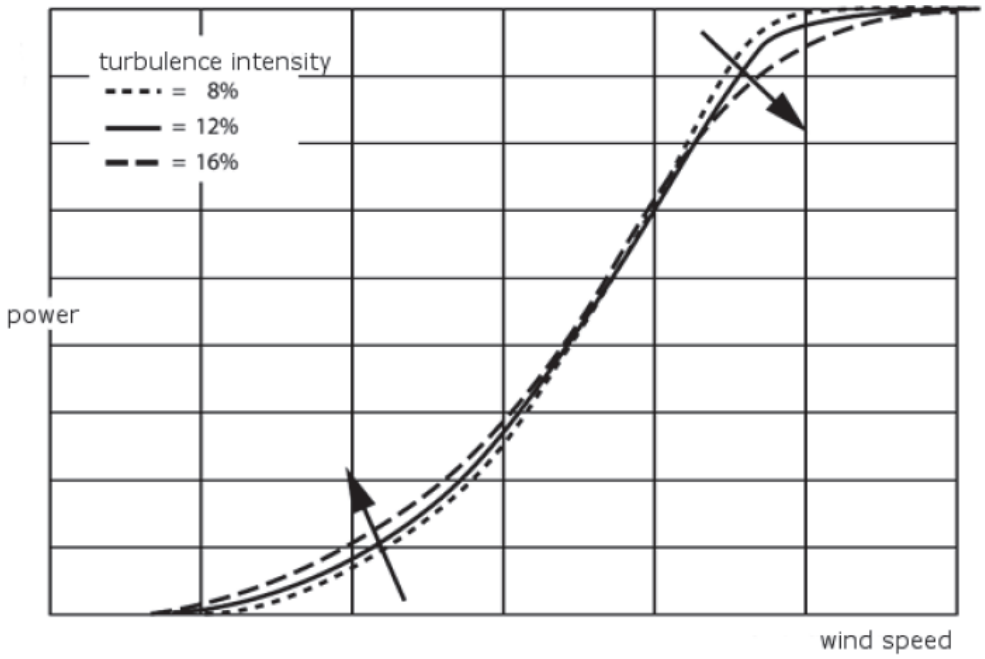

Fig. 4.6 Influence of TI on power production. [17]

As it follows from the Fig. 4.5 the power curve gets overestimated at low wind speed and underestimated at higher speeds. The reasons for this distortion are calculating error brought by data averaging (bin and 10 minutes' interval) and the relaxation of the power output caused by inertia effects of the wind turbine. The distortion effect is enhanced due to nonlinearity of wind speed and power relation. When the turbine works at the rated wind speed, any negative turbulent deviation will be perceived as a reduction in productivity, while deviations above the rated speed will not have a significant effect as the turbine operation above rated speed is limited. Similarly, when the turbine works at the wind speeds close to cut-in speed, any positive deviation on the contrary will be taken into account, whereas negative rejection will have no impact on turbine performance. Thus, the value of the curve will be lowered in the right-side bend and inflated on the left-side band.

In order to determine more accurately the relationship between the producing power and the corresponding wind speed in view of the turbulent component it is proposed to use the normalization method discussed in [19] and [20]. In mathematical interpretation overall wind speed can be written as the sum of mean ($\overline{WS}$) and turbulent (ws') wind speed values:

$$WS = \overline{WS} + ws' \tag{4.9}$$

The mean wind speed value $\overline{WS}$ is found as a time integral for the sample period T_s

$$\overline{WS} = \frac{1}{T_s}\int_0^{T_s} ws(t)dt \tag{4.10}$$

In wind energy applications, turbulence is usually described by its intensity, which can be found as a ratio of standard wind speed deviation (σ_{ws}) and wind speed average value:

$$TI = \frac{\sigma_{ws}}{\overline{WS}} \tag{4.11}$$

Power generated by wind turbine is directly proportional to the cube of wind speed. Thus, the mean cube wind speed value can be expressed from equation (4.9)

$$\overline{WS^3} = (\overline{WS} + \overline{ws'})^3 = (\overline{WS})^3 + 3 \cdot \overline{ws'} \cdot \left(\overline{WS}\right)^2 + 3 \cdot \overline{WS} \cdot \left(\overline{ws'}\right)^2 + \left(\overline{ws'}\right)^3 \tag{4.12}$$

In the equation (4.9), $\left(\overline{ws'}\right)^2$component is equal to 0 as floating of turbulent component has a symmetrical character and hence

$$\overline{WS}^3 = (\overline{WS})^3 + 3 \cdot \overline{WS} \cdot \left(\overline{ws'}\right)^2 = (\overline{WS})^3 \cdot (1 + 3 \cdot \frac{\overline{(ws')^2}}{(\overline{WS})^2}) \tag{4.13}$$

As it follows from equation (4.11)

$$\frac{\overline{(ws')^2}}{(\overline{WS})^2} = \left(\frac{\sigma_{ws}}{ws_i}\right)^2 = TI^2 \tag{4.14}$$

In this way, equation (4.13) will take a form:

$$\overline{WS^3} = (\overline{WS})^3 \cdot (1 + 3 \cdot TI^2) \tag{4.15}$$

As it seen from the equation (4.15), the flow with turbulence component (TI>0) has higher energy content.

Wind speed normalization for turbulence is done with a help of equation (4.15), and the value of normalized wind speed regarding turbulence component WS_{TI}^{norm} is found as:

$$WS_{TI}^{norm} = \overline{WS} \cdot \sqrt[3]{1 + 3 \cdot TI^2} \tag{4.16}$$

Wind shear

Wind flow directed along the surface of the ground will be slowed down due to interaction with the terrain surface. The speed deceleration, thus, will be the most pronounced in the lower layers of the flow, and as strong as heterogeneity of the contacting surface. This effect is known as vertical wind shear (wind shear).

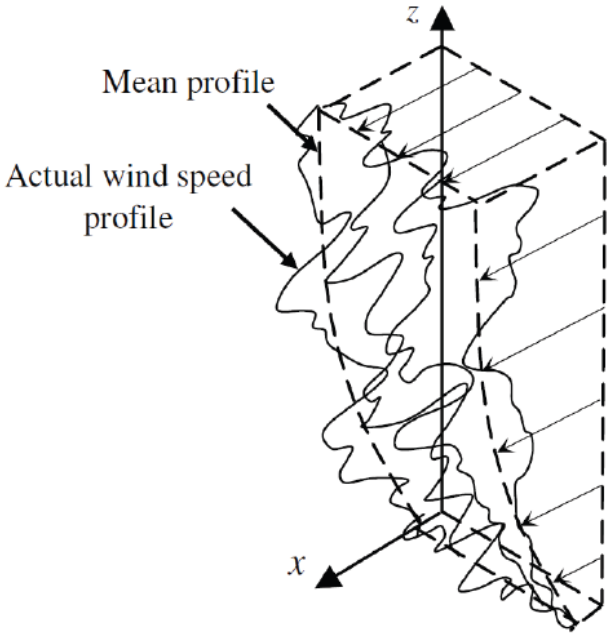

Fig. 4.7 Wind speed profile [20]

Spatial distribution of the wind profile including both the instantaneous and average values is shown in Fig. 4.7. As can be seen, the average wind speed rises with an increase in height.

In order to estimate the wind speed at certain height, the **wind profile power law** can be applied. The law establishes the relationship between wind speed and its height:

$$WS_z = WS_{ref} \cdot \left(\frac{z}{z_{ref}}\right)^{\alpha} \tag{4.17}$$

where WS_{ref} is a known wind speed measured at a reference height z_{ref} and WS_z is a target value at the height z. Wind shear exponent α is an empirical coefficient characterizing the topology of the terrain and atmosphere stability. The coefficient ranges from 0.11 - 0.14 (for neutral stability) up

to 0.4 (large city with tall buildings). In particular, for a more precise definition of wind shear exponent it is necessary to carry out measurements directly on the site of installations.

Another way to describe wind speed at a certain height is provided by logarithmic wind profile law. The approach requires much more detailed description of atmosphere stability and terrain characteristics that complicates its implementation. The law is presented below:

$$WS_z = \frac{ws^*}{\kappa} \cdot [\ln \frac{z-d}{z_0} + \psi(z, z_0, L)] \tag{4.18}$$

According to equation (4.18) wind speed height variation is a complex function where κ is a Kármán's constant, *d* is a zero plane displacement, *ws** is the friction velocity and ψ is a stability term depending on height *z*, surface roughness z_0, Monin-Obukhov stability parameter *L*.

The effect of the inhomogeneous distribution of wind power on height should be considered when evaluating the actual wind energy available at the rotor height. In the calculations it is proposed to use a method that is characterized by its simplicity and does not require additional information about turbine's placement or atmosphere conditions.

In order to determine the amount of energy in the wind flow it is proposed to use an equivalent wind speed method. The method allows to take into account the heterogeneity of the flow distribution along the rotor cross-section. For this purpose, cross-section is divided into parts, each of which is determined by the amount of contributed energy. Thus, this approach allows determine to more accurately the total flux of energy in view of its non-uniform distribution.

The method of equivalent wind speed normalization for wind shear is mainly adopted from [20] and [21].

Based on Betz's law the connection between the producing power and the speed of the wind flow passing through the wind turbine swept area is found as:

$$P' = \frac{1}{2} \cdot \rho \cdot A \cdot WS_{hub\ h.}^3 \tag{4.19}$$

$$P' = Cp \cdot P_{wind} \tag{4.20}$$

The relative power *P'* is calculated taking into account the power factor C_p, which shows the amount of wind energy available for power conversion. Coefficient is mainly dependent on geometrical characteristics of blade's profile. Theoretical maximum for C_p is 0.593. The other figures of the equation are *A* – turbine swept area, $WS_{hub.h}$ – wind speed at the hub height.

Taking into account that wind speed differs with height, the total relative power available for conversion can be found as a definite integral of wind kinetic energy taken along the turbine diameter

$$P' = \frac{1}{2} \cdot \rho \cdot \int_{Z_{hub\ h.}-R}^{Z_{hub\ h.}+R} crd(z) \cdot ws(z)^3 \, dz. \tag{4.21}$$

Integration limits are determined by geometry of turbine's rotor, where $Z_{hub\ h.}$ and R - turbine hub height and radius respectively, *crd* is a chord length forming by segment, $crd \in [0; 2R]$.

According to the vertical distribution the total energy available for conversion is dependent on the wind speed in every flux countered to the relevant height of the wind turbine rotor and can be found as a sum:

$$P' = \frac{1}{2} \cdot \rho \sum_{(i)} A_i \cdot WS_i^3 \tag{4.22}$$

$$P' = \frac{1}{2} \cdot \rho \sum_{(i)} A_i \cdot WS_i^3 = \frac{1}{2} \rho \cdot A \cdot WS_{eq}^3 \tag{4.23}$$

WS_i is a segment wind speed of the flux countered to the relevant segment A_i of the total area A. WS_{eq} is an equivalent wind speed found as a superposition segment wind speeds.

Based on equation (4.23) WS_{eq} can be found as sum of all wind streams interacting with turbine rotor:

$$WS_{eq} = \left(\sum_{(i)} WS_i^3 \cdot \frac{S_i}{A} \right)^{1/3} \tag{4.24}$$

To specify segment separation of turbine swept area the following levels of 69, 80, 91, 102 and 113 m available from Lidar were taken. The choice was made using the heights attributable to the central area of the turbine rotor which have to have the greatest impact as this effect is getting lower at the edges – the ratio $\frac{S_i}{A}$ becomes less significant. At the same time consideration of every next height leads to the reduction in data available for the analysis due to the wind data availability and direction filtering. By this way the explored area A has been divided on 5 semisegments. The resulting separation is presented in Fig. 4.8.

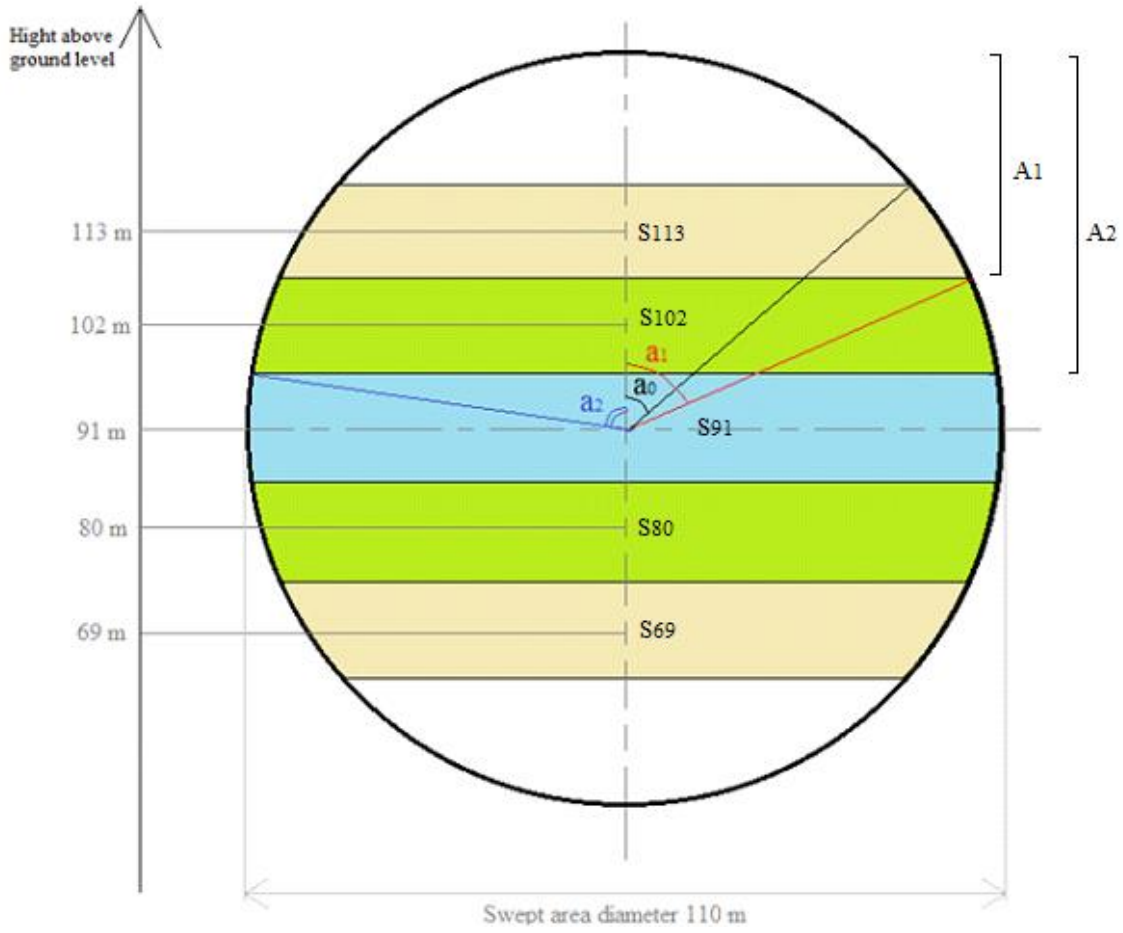

Fig. 4.8 Segment separation of turbine swept area

The diameter of turbine rotor is 110 m. Then its swept area A^{sw} is equal to 9503.32 m^2.

To find the area of each semisegment in the beginning it is necessary to determine the areas of the corresponding segments A_1 and A_2.

The angle a_1' is equal to the half of corresponding central angle α_1 and can be found as

$$\cos a_1' = \frac{h_1+h_2}{R} = \frac{5.5+11}{55} = 0.3 \qquad (4.25)$$

$$a_1' = 72.54^{\circ}$$

$$\alpha_1 = 145.08^{\circ}$$

where h_1 is equal to 11 m – measuring height step of Lidar radar, h_2 is a half-step.

Using a known expression, we determine the first segment area:

$$A_1 = \frac{1}{2} \cdot R^2 \cdot (\alpha_1 - \sqrt{(1 - \cos^2 \alpha_1)}) \tag{4.26}$$

$$A_1 = 2964.03 \text{ (m}^2\text{)}$$

By the same token central angle $\alpha_2 = 2 \cdot a_2'$ and segment area A_2 are found as follow:

$$\cos a_2' = \frac{h_1}{R} = \frac{5.5}{55} = 0.1$$

$$\alpha_2 = 168.52^{\text{O}}$$

$$A_2 = \frac{1}{2} \cdot R^2 \cdot (\alpha_2 - (\sqrt{(1 - \cos^2 \alpha_2)}) \tag{4.27}$$

$$A_2 = 4147.58 \text{ (m}^2\text{)}$$

The total area excluded from consideration (white zone) is found similarly

$$\cos a_0' = \frac{h_1}{R} = \frac{5.5 + 11 + 11}{55} = 0.5$$

$$\alpha_0 = 120^{\text{O}}$$

$$A_{exc} = 3715.52 \text{ (m}^2\text{).}$$

Finally, the total considered area A is found as the difference between turbine swept area and the total excluded area what is equal to 5787.8 m^2. In this way, obtained values of the wind power at the choice of partial segmentation can differ and be a little lower than at wind shear normalization for a whole radius of the turbine, even though within the considered reference power calculation this divergence should not have a critical character.

As follows from Fig. 4.8, semisegments S_{69} and S_{113} can be found as the difference between area A_1 and A_{exc}. Semisegments S_{80} and S_{102} - as the difference between area A_2 and A_1. Semisegment S_{91} is then found as the rest area of the considered region. The result of the calculations is given in the Table 4.1

Table 4.1 Calculation result

Semisegment area	S_i value, m^2	S_i/A ratio
S_{69} and S_{113}	1106.13	0.19
S_{80} and S_{102}	1183.55	0.2
S_{91}	1208.16	0.21

Thus, equivalent wind speed WS_{eq} can be found by equation (4.24) with a help obtained ratio values.

4.4.3 Data preprocessing overview

All the steps applied on data preprocessing are collected and listed in Table 4.2.

Table 4.2 Data preprocessing steps

Filtration	
Filter	Filter boundaries
Wind data availability	>60%
Wind direction	Block sector from 348 to 183 degrees
Minimal generator speed	1000 rpm
Normalization	
Air density	$WS_{norm_i}^{hub\ h.} = WS_i^{hub\ h.} \cdot (\frac{\rho_{air}^{hub\ h.}}{\rho_0})^{\frac{1}{3}}$
Turbulence intensity	$WS_{TI}^{norm} = \overline{WS} \cdot \sqrt[3]{1 + 3 \cdot TI^2}$
Wind shear	$WS_{eq} = \left(\sum_{(i)} WS_i^3 \cdot \frac{S_i}{A} \right)^{1/3}$

The resulting impact of preprocessing is presented in Figure 4.9. Blue dots depict unprocessed data, whereas red ones are for data normalized for air density, turbulence intensity and wind shear.

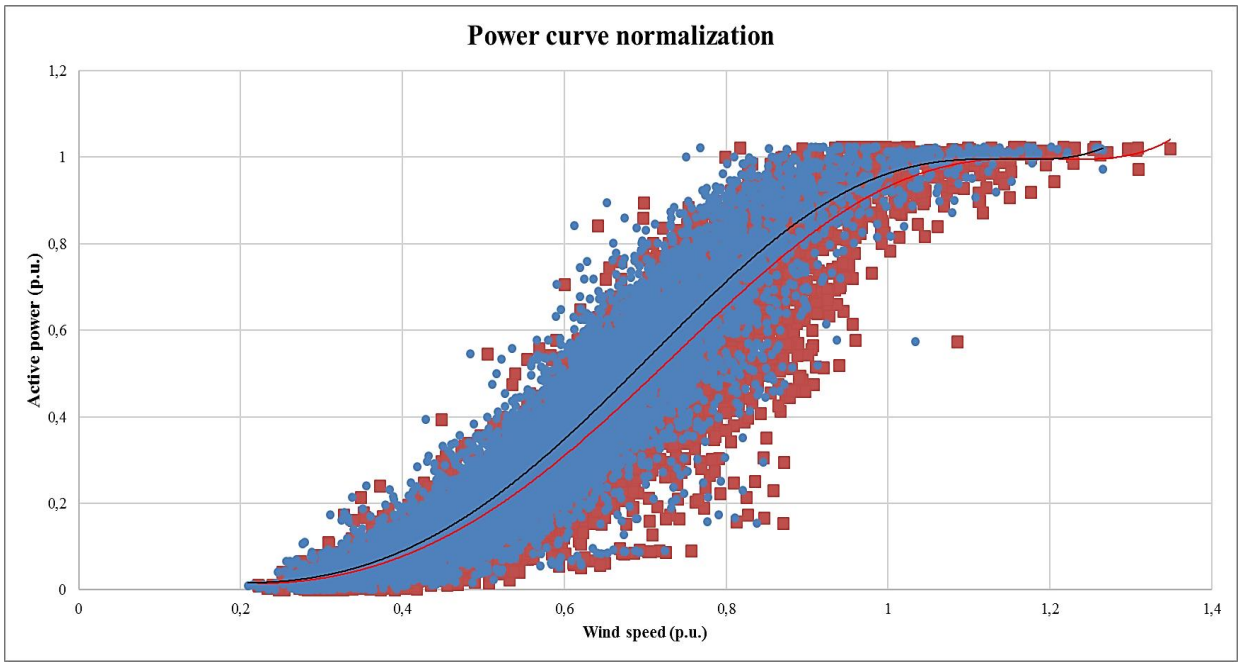

Fig. 4.9 Power curve normalization

The effect of normalization is clearly shown by trend lines built for both unprocessed (blue dots, black trend line) and normalized (red dots, red trend line) data. As is seen from the plot, the normalized trend line is shifted to the right compared with the original values measured by Lidar radar. This shift is not constant and depends on parameters used for normalization.

5 Results presentation

As follows from subchapter 4.2 the method of proposed indirect ice detection is using an assumption that at the presence of ice, the output power level of turbine has to be lower than in case of normal operational conditions.

Before the analysis, the data has been preprocessed. The process of data filtration and normalization is in detail described in subchapter 4.4.

In short, first the data was filtered for parameter's availability, wind direction and generator rotational speed in order to discard unreliable information from the calculations.

Then, selected wind speed data was normalized for air density, turbulence intensity and vertical wind shear. The process is discussed in subchapter 4.4.2, equations used at these stages are also presented in Table 4.2

Having defined the reference levels for each wind speed bin, these values were correlated with each value in the bin. As a result, the relation of actual and reference power output ($\frac{P_{WS_i}}{P_{WS_i}^{ref}}$) was obtained, showing how much and in which way the performance of the turbine differs from the desired value at the certain moment of time. It is assumed that the received reference value represents a certain level at which operation of the turbine is not reduced as a result of ice accretion. Thus, any negative deviation in productivity will be perceived as influence of icing. However, it should be noted that calculations carry evaluative character as to determine exactly the impact of icing on the turbine performance is not possible. Determination of the reference level can be affected by the influence of the measurement and calculation errors. Thus, all the received values should be taken as indicative values, which describe the overall trend in turbine performance degradation. In more detail the issue is discussed in conclusion part on the carried analyses.

The whole process of data analysis was made using Excel software. The data sources used for calculations are Lidar and SCADA. The results of the analysis were compared with the information available from the ice sensors and camera (mounted on the nacelle of the turbine).

5.1 Results

On the analysis results, characterization of wind turbine operation has been received, where each value of wind turbine output is determined as a deviation from the reference value. As well as it was expected, continuous intervals of time at which productivity of the turbine remains much lower than the established values have been obtained. Some of the most notable examples are shown in this chapter.

Case 1

The performance deterioration of the turbine from October 25 to October 26 2014 are shown in Fig. 5.1.

Hereinafter, the ambient temperature is shown in orange. Green and blue lines are for the ice alarm signals from the A and B ice sensors. Camera signal is depicted by purple line. At the same time, the signals from both sensors and camera aren't tied to neither an axis of power deviation nor to the temperature axis, and only indicate the presence and extent of the respective signals. The red vertical bars display $\frac{P_{WS_i}}{P_{WS_i}^{ref}}$ ratio, expressed as a percentage. The bars refer to the deviation of actual generated power (GP) over average level axis. Wind speed for every case is shown separately in the same time scale.

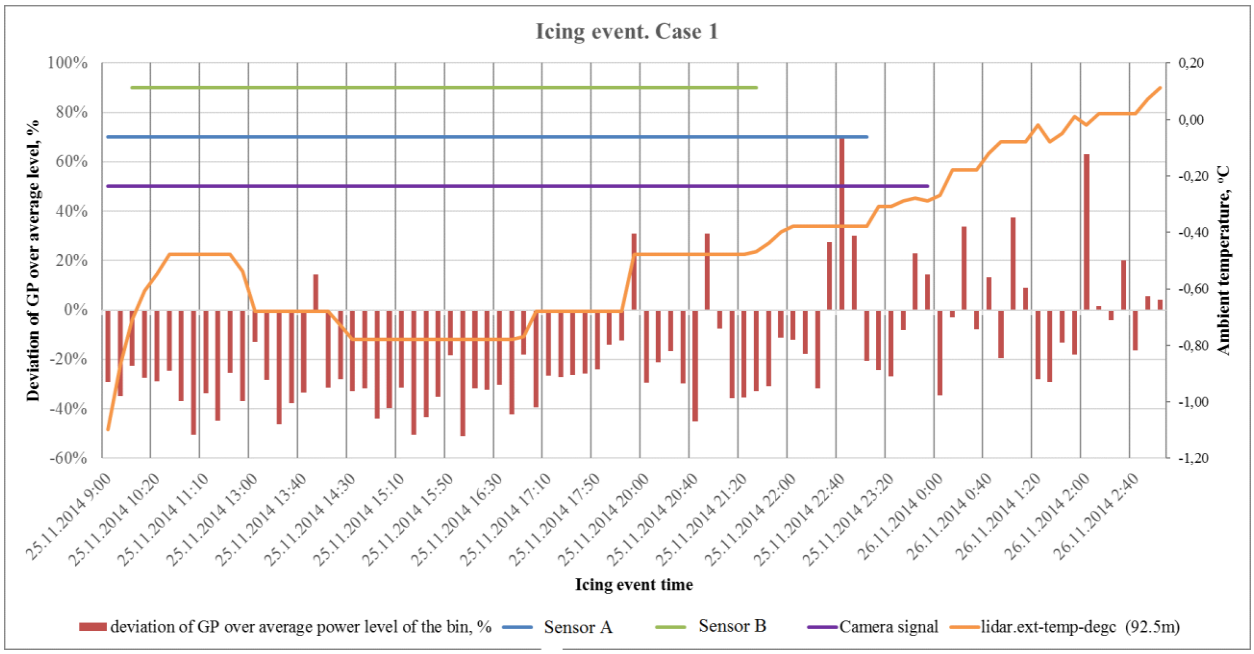

Fig. 5.1 Icing event. Case 1

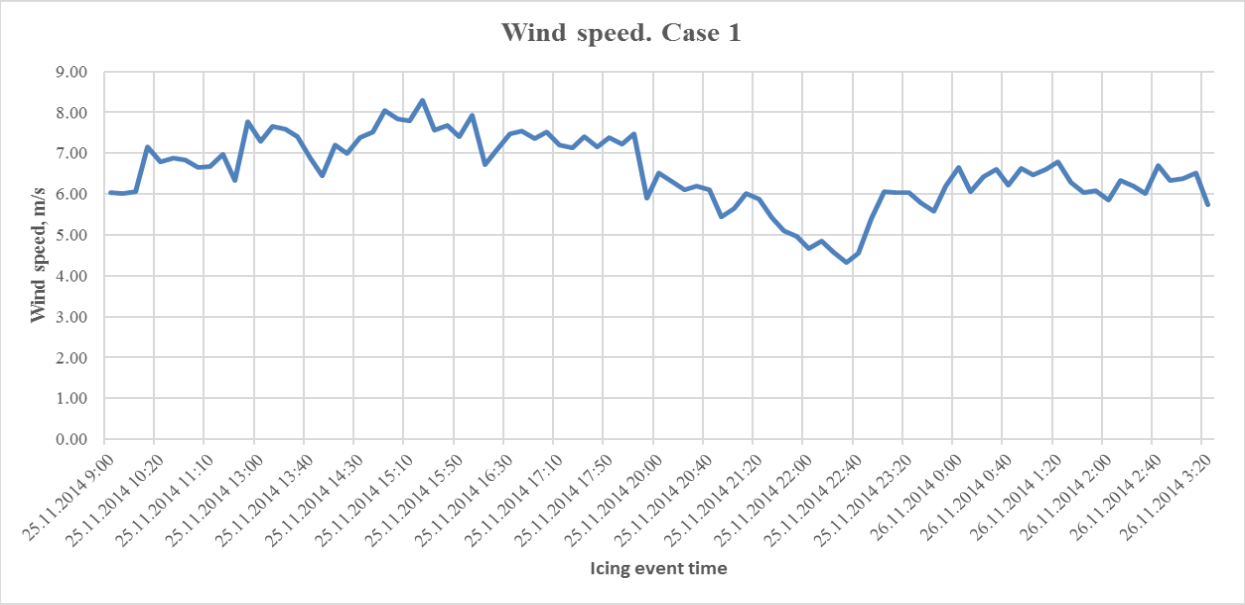

Fig. 5.2 Wind speed. Case 1

As it follows from Fig. 5.1, the performance of the turbine is lowered almost entirely from 9 am to 10 pm and starts to recover after that. At the same time, during this period there is a negative temperature close to 0 degrees, which is starting to grow in 2 hours before the turbine performance starts to get at normal level and before the camera and ice sensors stop sending ice alarm signals. Throughout the time the conditions are favorable for the formation of ice. Wind speed remains higher than turbine cut-in speed (Fig. 5.2). Here and after (as it was mentioned and described in subchapter 4.2) positive deviation in power can be received due to partial consideration of aerodynamic power at the stage of wind shear normalization. Another reason could be hidden in reference calculation error. In more detail the issue is discussed in the conclusion to this chapter.

Case 2

The performance deterioration is observed during the dates of 28.11 and 29.11.2014. Operation of the turbine under possible icing event is shown in Figure 5.3.

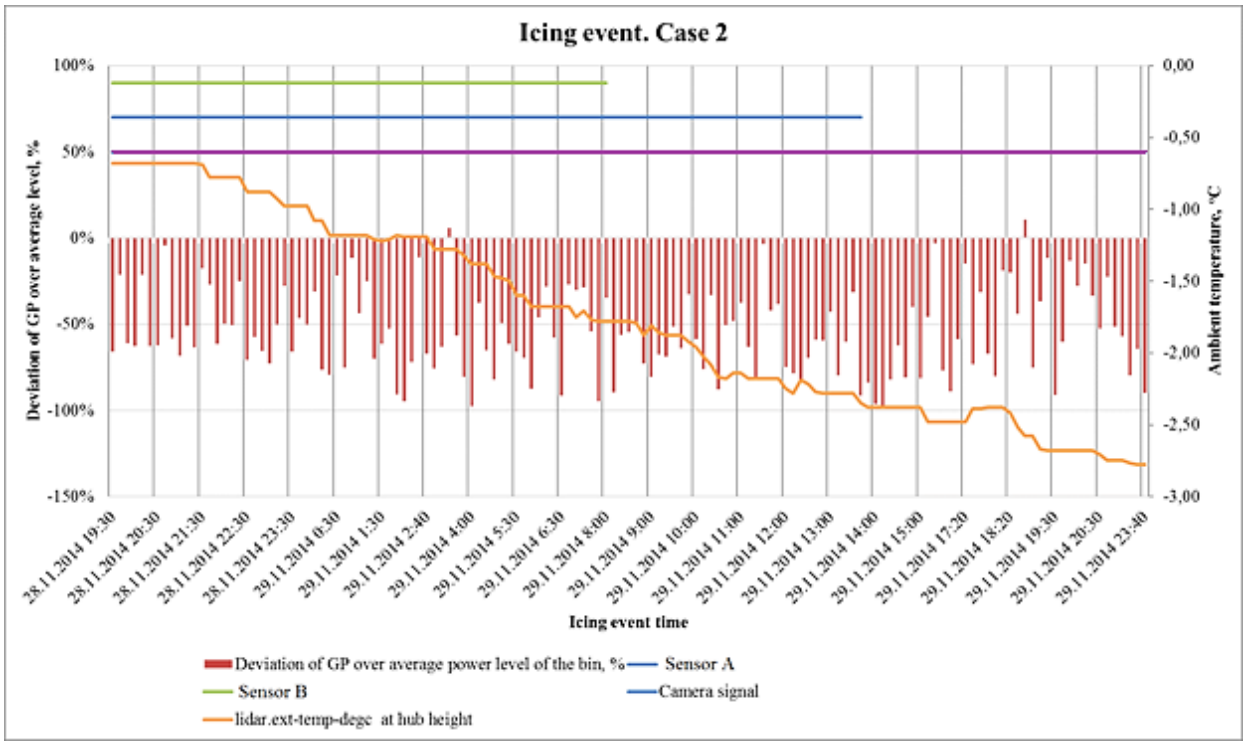

Fig. 5.3 Icing event. Case 2

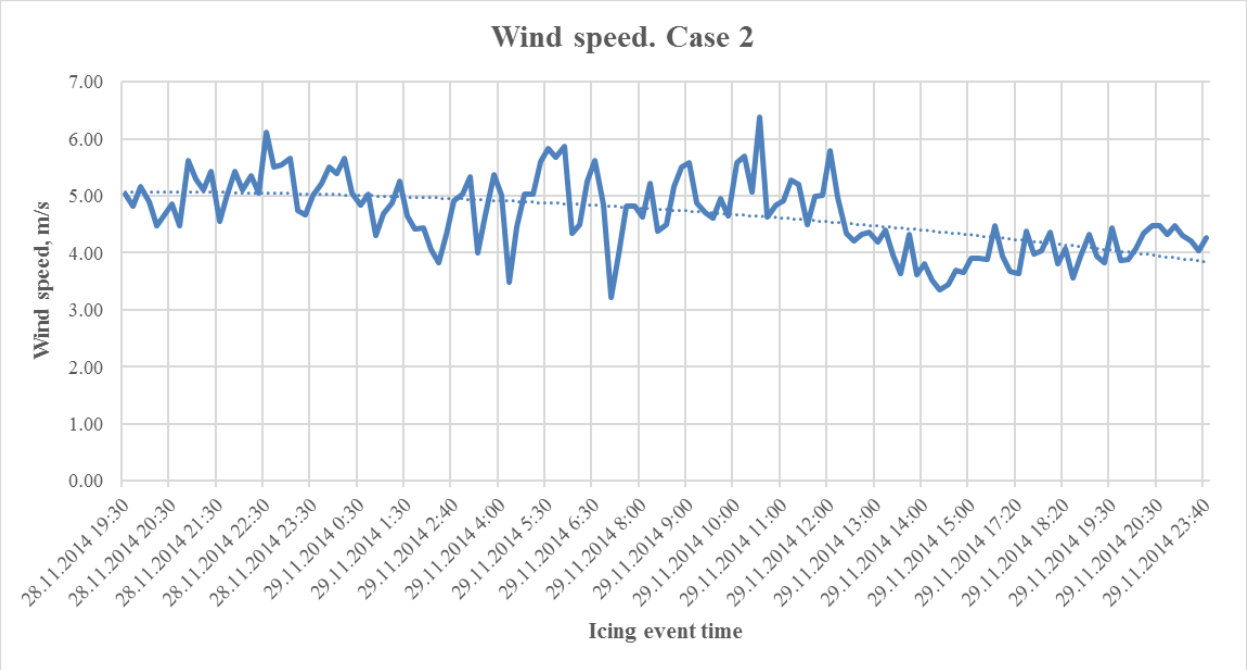

Fig. 5.4 Wind speed. Case 2

Throughout the entire length of time a reduction in turbine efficiency is observed. Weather conditions are favorable for ice formation: humidity of the air is 100 %, temperature remains negative and gets lower. During the period (especially at the end) wind speed is close to cut-in speed (4 m/s) and even gets lower.

Continuous decline in turbine performance can be explained by the presence of ice formed at the beginning of the considered period (marked by ice sensor alarm signals). The sensors stop giving ice alarm at the end of the period, but the camera shows the ice also for the next day, while temperature continues to decrease.

Case 3

The performance of wind turbine is lowered during the period from 9.02. to 10.02.2015 Operation of the turbine under possible icing event is shown in Fig. 5.5.

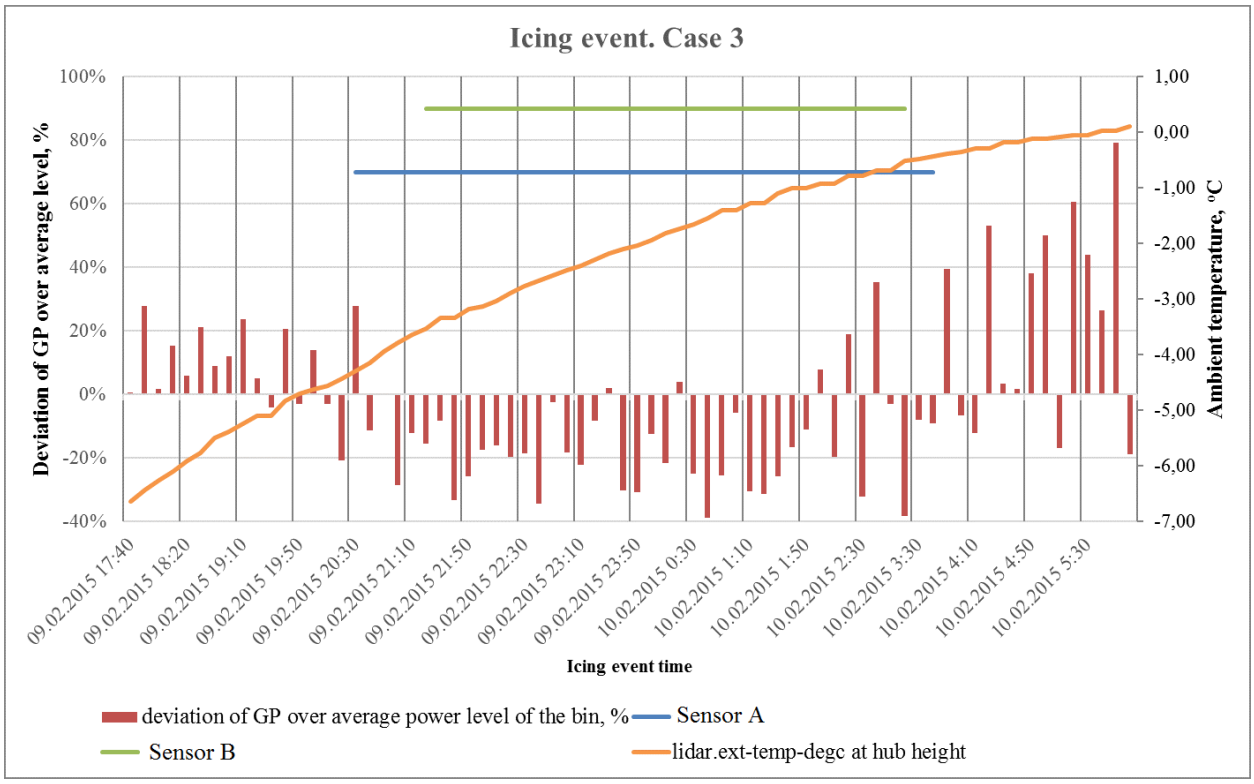

Fig. 5.5 Icing event. Case 3

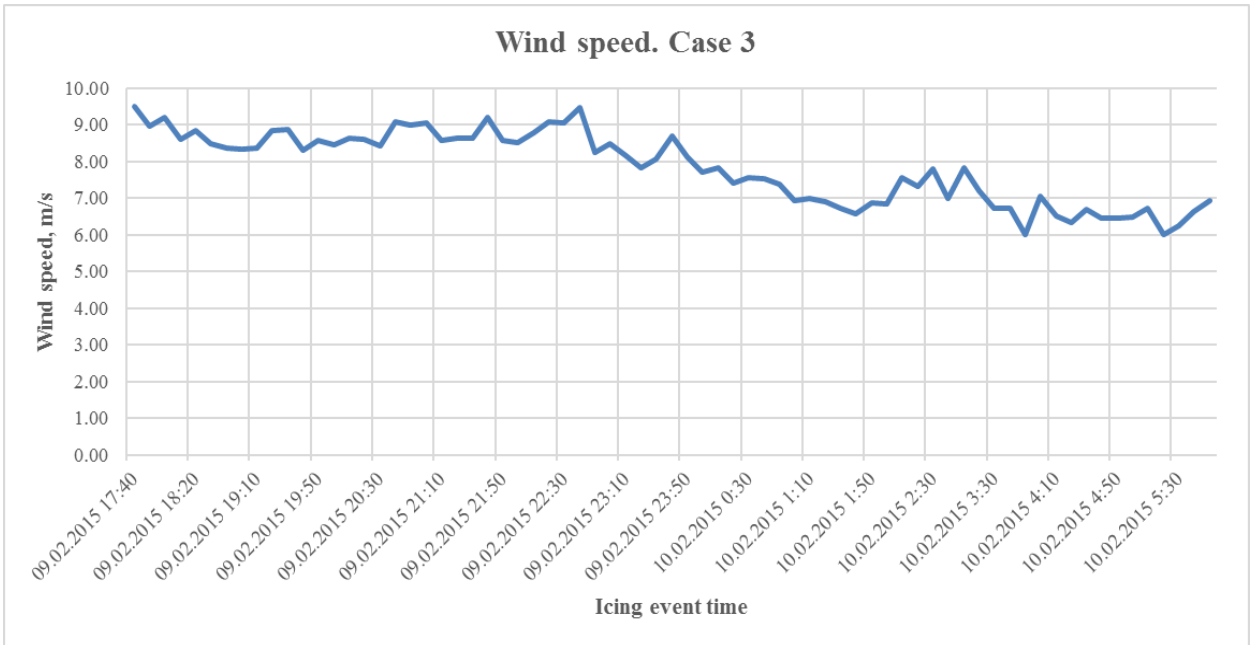

Fig. 5.6 Wind speed. Case 3

The power production is reduced from the evening until the morning. Temperature rises and becomes positive in the same morning. Ice sensor signals are on during the time of power gap. Air humidity is high - 98-99 %. Thus, it can be said that weather conditions are preferable for ice accretion during the night, while at the morning ice is probably melted. In turn, and as noted earlier, there is no signal from the camera due to the inability to determine the ice in the dark.

Case 4

The drop in power production is observed during the period from 22.03. to 23.03.2015. Operation of the turbine under possible icing event is shown in Fig. 5.7.

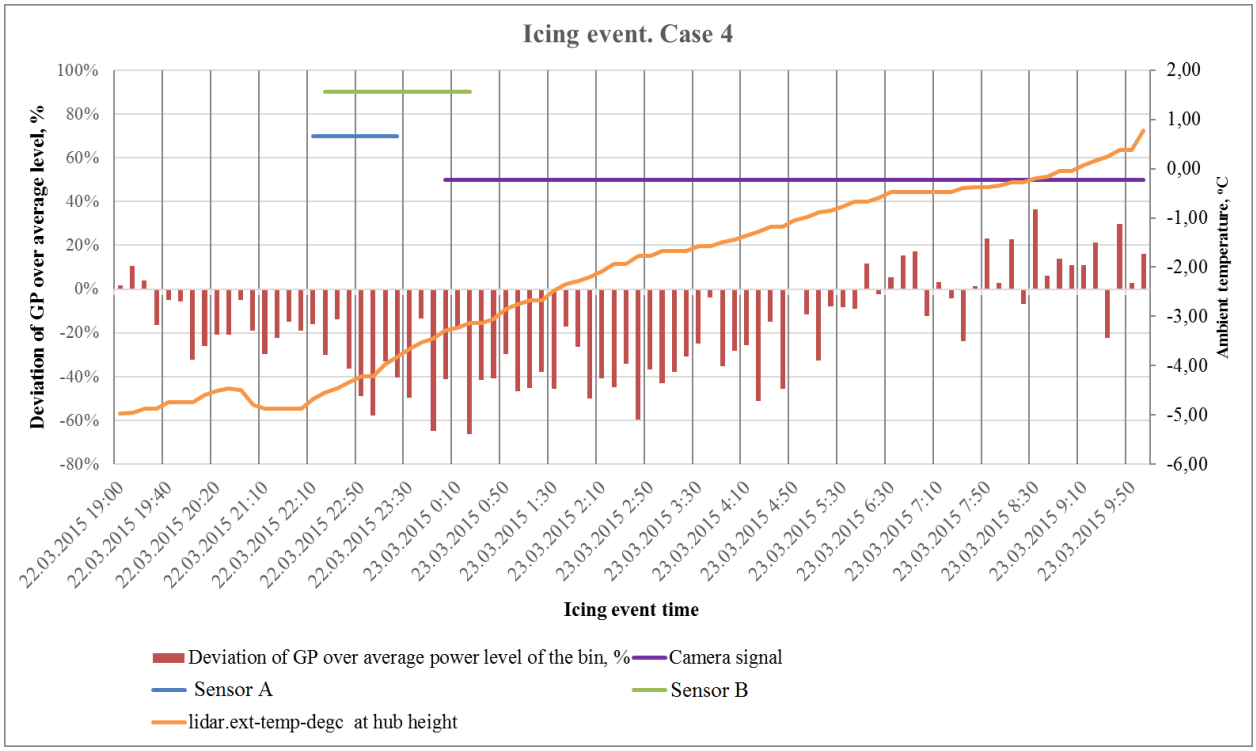

Fig. 5.7 Icing event. Case 4

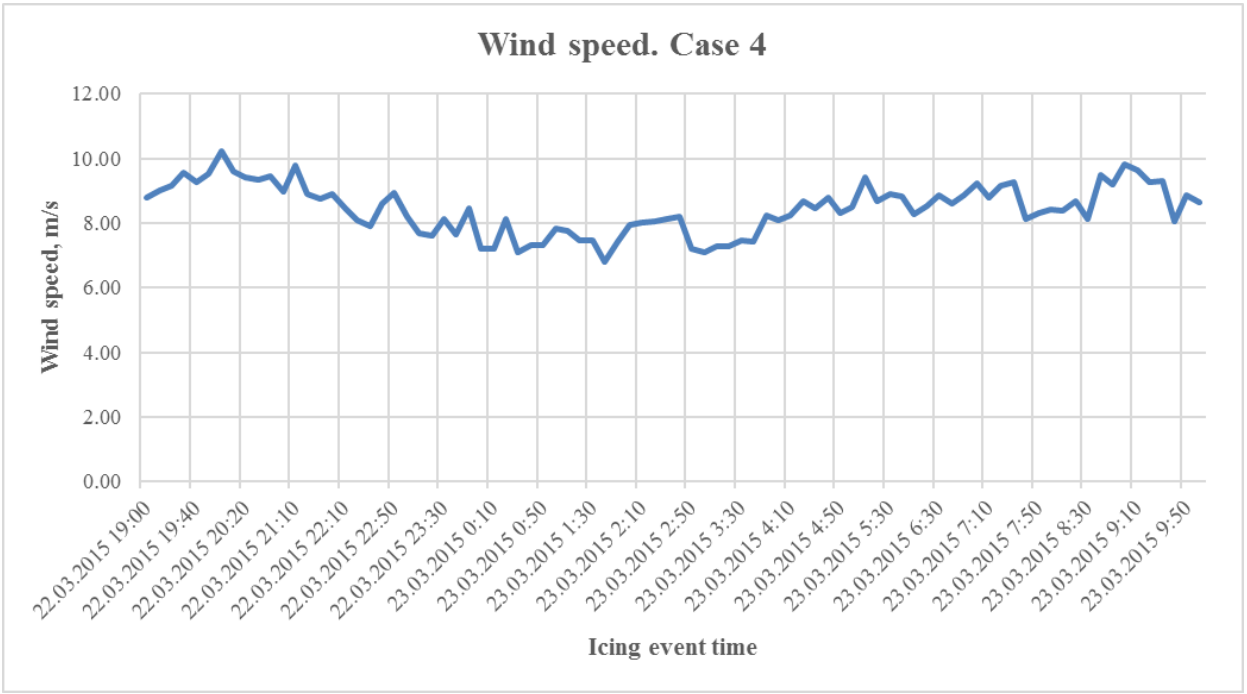

Fig. 5.8 Icing event. Case 4

The power ratio gets considerably negative approximately 2 hours before the first ice alarm and remains low 5 hours after the last ice alarm. As previously mentioned, the difference in time may be caused by the fact that ice sensors can operate with a delay because of their positioning 50 meters lower than the maximum height of the passage of the turbine blades over rotation (where the temperature is normally lower). The camera signal appears only on the day after the signals from the ice sensors, which is likely due to the inability to monitor the ice in the dark time. At the time when power ratio gets positive sign temperature is close to zero and becomes positive. A little mismatch with temperature change can be led by temperature measurement and/or estimation error. Wind speed is 8 m/s on average and remains upper than cut-in level for entire period (Fig. 5.8).

5.2 Power loss calculation

Further, calculations for definition of quantitative indices of decline in production of the turbine for the considered cases have been made. The calculation results are presented in Table 5.1. All calculations carry only evaluative character as to determine exactly the impact of icing on the turbine performance is not possible. Thus, all the received values can be taken only as indicative values, which describe the overall trends.

The table includes the following parameters:

- Average decline in production for the period - average level of productivity degradation of the turbine for the whole period of the case.
- Power loss, % – shows the amount of uncollected energy expressed as a fraction of the total expected amount;
  Power loss level is calculated as

$$P_{loss} = \sum(1 - \frac{P_{WS_i}}{P_{WS_i}^{ref}}) \quad (5.1)$$

  where

  $P_{WS_i}^{ref}$ – expected (reference) power output of the 10-minutes interval;

  P_{WS_i} – actual power output of the 10-minutes interval;

  P_{loss} – total power loss of the case.

- Power loss;
- Period length, h – duration of the ice event.

Table 5.1 Quantitative indices of the turbine performance during ice event

Case	Case length, h	Average decline in turbine power for the period, %	Power loss, %
Case 1	14.5	-18	33
Case 2	23	-55	59
Case 3	11	-6	5
Case 4	14.33	-18	16.5

As follows from the table, during the operation under ice event, turbine productivity considerably decreases, while power losses can reach the level of more than a half from the expected output. Power loss is estimated as a total effect of decline in turbine production in comparison with the output level available during the work on reference power values for the same period of time (eq. 5.1). Average decline in energy production is calculated as the average level of turbine productivity reduction (shown in case pictures by red vertical bars) for the considered time interval.

In order to obtaining more exact characteristics, it is necessary to increase both interval of observation, and accuracy of measurements by reducing a measurement sampling step of wind speed.

At the next stage of the analysis, similar calculations were carried out for the entire operational period (November 2014 to April 2015) of the turbine including:

- time intervals when ice detectors have detected ice. Calculations are made for entire analyzed period and only for the time when ice alarms are received. The results are shown in Table 5.2.
- time intervals when negative power deviation is identified. Calculations are made under assumption that every negative deviation in power production is caused by ice accretion. The results are given in Table 5.3.

Table 5.2 Quantitative indices of the turbine performance when ice detectors have detected ice.

Operational period, h	Average decline in turbine power, %	Power loss, %
74	-26	20.73

Operation of the turbine for the entire period when signals of ice detectors are received is 74 hours. During this time the average decline in production was 26%.

Table 5.3 Quantitative indices of the turbine performance when negative power deviation is observed

Operational period, h	Average decline in turbine power, %	Power loss, %
796,5	-22	18

By results of an assessment of turbine performance degradation at which any negative deviation was considered as a consequence of ice accretion follows that the average decline in production for entire considered period makes 22% that corresponds to 18% of power loss.

Finally, in order to determine feasibility of the calculated values of power loss, the analysis result was compared with the results obtained in similar studies. The review of the works is presented in Table 5.4.

Table 5.4 Other studies review

Authors	Year of publication	Topic	Power loss
Erik Hellström [22]	2013	Development of a model for estimation of wind farm production losses due to icing	6.4 % of annual possible production
Dahlberg, Jan-Åke & Thor, Sven-Erik [23]	2011	Internal report A, Vattenfall Vindkraft AB	8.4 % of annual possible production
Ville Turkia, Saara Huttunen, Tomas Wallenius [24]	2013	Method for estimating wind turbine production losses due to icing	From 4 to 36 % for different modelling situations

By results of the comparative analysis it is possible to conclude that the received value of losses of 18% is more than twice higher than the results of similar calculations in [22] [23] (6.4% and 8.4 % of annual possible production). At the same time the results received for different modelling cases in [24] are close to the values obtained for the considered cases in current work.

Conclusion on the carried analyses

In the course of the analysis of turbine operation regarding its performance in the icing conditions has been carried out and the appropriate level of power loss has been defined. As a result, the time intervals, defined as operation of the turbine in icing conditions were identified. By comparison to data of sensors and meteorological information it is possible to draw a conclusion that in the majority of cases the determined periods coincide. Some such cases were taken as an examples for description. The results of chapter 5.1 show that the indirect ice detection method used in the study is applicable in ice detection, at least when significant amount of ice is accreted on the blades. The data obtained in loss estimation are mainly consistent with the results of similar studies. Nonetheless the loss estimation results are somewhat higher. It should be noted that the main object of the carried-out analysis is identification of consecutive continuous deviations in turbine performance. Further these cases are considered for the presence of conditions favorable for ice accretion. However, the deterioration of performance may also be caused by the following factors:

- Presence of failure at which the turbine continues to operate at reduced capacity (Pitch control error, bearing deformation etc.);
- Low wind speed intensity;

  During the operation of the turbine in conditions of low wind intensity operation of the turbine will be followed by frequent stops. In this case, the energy produced will be reduced due to operational brakes and relaxation process (acceleration and deceleration) of turbine mechanism.
- Reference value determination error.

  There was comparably small amount of data available for wind speed bins when turbine operates at the speeds close to cut-off level. Thus, determination of reference values for such cases may suffer. One way to obtain more accurate reference power values is to increase the period under consideration.
- Operation of the turbine under derated control strategy

  In the conditions of extremely low temperatures, the turbine is operated by derated control strategy at which the turbine productivity is intentionally lowered. Throughout the analyzed period there were just a couple of days at which the temperature reached the appropriate low level. Therefore, in this study the impact of this mode of operation is not taken into account that could make minor adjustments to the results of the analysis.
- Wind speed averaging error;

  It is known that the wind speed is a parameter with high volatility. It is logical to assume that when the turbine at speeds works at the wind speeds close to cut-in value, it is likely

that in the ten-minute interval there will be a large number of instantaneous wind speed values below the cut-in level, that cannot be expressed evidently in the ten-minute average value. For example, in the sample of 10 minutes' instantaneous wind speed may not exceed cut-in value for 8 minutes and rise over at the end of the interval. In this case, the calculated average value of wind speed may be higher than turbine cut-in speed, although it is obvious that the level of produced power will be below the expected level. This effect is especially pronounced when the turbine operates at the minimum speeds. Thus, at similar calculation of power loss during the operation of the turbine at speeds over 6 m/s the estimated level of average decline in production decreases from 21% to 18%.

For the effect of these factors an obtained value of power loss (-18%), in a case of considering only the impact of icing can to be represented by a smaller value. However, it is impossible to predict the exact reduction.

6 Conclusions and further research ideas

In this study, common problems associated with the operation of wind turbine in cold climate along with types of icing and the process of ice formation were briefly discussed. Direct and indirect methods of ice detecting were also analyzed and compared.

Next the method of indirect ice detection has been proposed and the analysis of power losses caused by estimated ice is carried out. The basic idea of the analysis was based on the assumption that icing process is not instantaneous in nature, and hence the effect on turbine performance should be observed in the form of long-term and sustainable decline in production. Thus, to detect icing events it was necessary to identify such sequential performance degradation.

By means of the proposed method the periods of time when turbine operation is constantly lowered were detected. By comparison of results of the analysis with meteorological information and ice sensors' data it has been established that in the majority the considered cases were followed by signals of sensors. At the same time the weather conditions were favorable for ice formation. Thus, by results of the carried-out work it is possible to conclude that the offered method of indirect ice detection is quite efficient and operable.

Among the advantages of the method it is possible to mark out its simplicity and the absence of the need for building an aerodynamic model of the turbine.. The main drawback is the inability with guarantee to determine icing events resulting from the use of average data in the calculations. The associated problems of low wind speed intensity, wind speed averaging error, reference value determination error and impossibility to isolate the influence of operational failure in the analyses of data were revealed and discussed.

Another aim of the study was to estimate the losses caused by the turbine icing. Calculations have been carried out both for the concrete set of cases, and for determination of the general level of losses for the entire period of observation. According to information received overall level of losses over the whole period is not exceeding 18% of total amount of possible production. This value is generally comparable to the results obtained in similar studies. Possible reasons for the discrepancy in calculated values of total power losses are also considered. The assessment of losses carries indicative nature, the results of which strongly depend on the characteristics of the research object (location and climate, the structural features of the turbine) and on the methods of calculation.

As the main ideas on improvement of reliability of the considered method it is possible to allocate three directions:

- Increase in number of observed objects;
  The reliability of the results can be improved and checked by analyzing the work of a larger number of turbines also working in another wind farms.
- Increase the period of observation;
  By analyzing a longer period, it is possible to get more precise reference values for turbine power production.
- Increase an accuracy of reference values determination.
  Another potential opportunity to improve the accuracy of calculation of the reference power levels is to isolate the influence of the values obtained during operation of the turbine in icing conditions. But this at variance, requires accurate information about ice events, which can be obtained by using blade-mounted ice detectors.
- Increase measurement accuracy;
  The accuracy of the calculations can be improved by analyzing measurements with shorter sampling rate. The key analyzed parameter is wind speed, which is characterized by high volatility. Therefore, use of average 10-minutes data in certain cases can bring considerable distortion of result. A good example that demonstrates this effect (ten-minute sample) on power output estimation is given in [17]: “At a uniform wind speed of 6 m/s in 10 minutes, a representative test turbine produces 132 W/m^2. At 12 m/s over 5 min and windless in the other 5 min, the average is also 6 m/s, but 528 W/m^2 are generated”.

7 References

1. IEA WIND 2013 Annual Report, August 2014 http://www.ieawind.org/annual_reports_PDF/2013/2013%20AR_small_090114.pdf, [Retrieved 23.6.2015].
2. World Wind Resource Assessment Report, 2014. Available: http://www.wwindea.org/, [Retrieved 23.6.2015].
3. GWEC Global Wind Energy Council. Available: http://www.gwec.net/global-figures/graphs/ , [Retrieved 23.6.2015].
4. American Wind Energy Association. Wind Energy and Wildlife: The Three C's. Available:http://web.archive.org/web/20060131235116/http://www.awea.org/pubs/factsheets/050629-ThreeC'sFactSheet.pdf , [Retrieved 23.6.2015].
5. Antoine Lacroix and Dr. James F. Manwell, "Wind Energy: Cold Weather Issues", University of Massachusetts at Amherst, June 2000. Available: http://www.ecs.umass.edu/mie/labs/rerl/research/Cold_Weather_White_Paper.pdf, [Retrieved 31.7.2016].
6. A. Heiman, R. Catting, and B. Calpine, Recommendations for Meteorological Measurements under Icing Conditions, IWAIS XIII, Andermatt, 2009. Available: http://iwais.compusult.net/html/IWAIS_Proceedings/IWAIS_2009/Session_4_cost_727_wg2/session_4_heimo.pdf , [Retrieved 15.8.2015].
7. Sukhoi superjet 100. Available: http://superjet100.info/wiki:obledenenie , [Retrieved 11.3.2016].
8. Kelly Aerospace. Available: http://www.kellyaerospace.com/wind_turbine_deice.html, [Retrieved 11.3.2016].
9. Expert group study on recommended practices, 13. Wind energy projects in cold climates, 1st ed., 2011, Available: http://www.tuulivoimayhdistys.fi/filebank/195RP13_Wind_Energy_Projects_in_Cold_Climates_Ed2011.pdf , [Retrieved 22.4.2016].
10. M.C. Homola, Impacts and causes of icing on wind turbines, Windenergy in the BSR, 2005.Available: http://ansatte.hin.no/mch/documents/Wind%20energy%20BSRImpacts%20and%20causes%20of%20icing%20on%20wind%20turbines.pdf, [Retrieved 10.5.2016]
11. Norwegian Meteorological Institute and Norwegian Broadcasting Corporation. Available: https://www.yr.no/place/Finland/Southern_Finland/Lappeenranta/statistics.html, [Retrieved 14.2.2015]

12. Permitting Setbacks for Wind Turbines and the Blade Throw Hazard, California Wind Energy Collaborative, 2005. Available: http://centralbedfordshire.gov.uk/Images/wind-farm-tech_tcm3-13230.pdf
13. Victor Carlsson, Measuring routines of ice accretion for Wind Turbine applications, Master's thesis, Sweden, 2010. Available: http://www.divaportal.org/smash/get/diva2:370953/FULLTEXT01.pdf, [Retrieved 18.4.2016].
14. Finnish Wind Atlas. Available: http://www.tuuliatlas.fi/en/
15. Fault Diagnosis Methods for Wind Turbines Health Monitoring: a Review. Available: https://www.phmsociety.org/sites/phmsociety.org/files/phm_submission/2014/phmce_14_026.pdf , [Retrieved 17.6.2016].
16. Annual of the ICAO Standard Atmosphere (extended to 80 kilometers (262 500 feet)) (Third ed.). International Civil Aviation Organization. 1993. ISBN 92-9194-004-6. Doc 7488-CD.
17. Katharina Eichhorn "The change of power curves as a function of various meteorological parameters" Master Thesis in Atmospheric Sciences. University of Innsbruck, 2013Sharma, S., & Mahto, D. (2013). Condition monitoring of wind turbines: a review. International Journal of Scientific and Engineering Research, 4(8), 35-50.
18. T. Burton, N. Jenkins, D. Sharpe, and E. Bossanyi, Wind energy handbook. John Wiley & Sons, 2011.
19. J.Wagenaar and P. Eecen, "Dependence of power performance on atmospheric conditions and possible corrections," p. 12, ECN Windenergie, March 2011. Paper presented at the EWEA 2011.
20. H.M. Villanueva Lopez «The Illusion of Power Curves Understanding TI, Shear, and Atmospheric Stability in Power Performance», March 4, 2014
21. R. Wagner, «Accounting for the speed shear in wind turbine power performance measurement»
22. Erik Hellström «Development of a model for estimation of wind farm production losses due to icing», 2013
23. Dahlberg, Jan-Åke & Thor, Sven-Erik, Internal report A, Vattenfall Vindkraft, 2011
24. Ville Turkia, Saara Huttunen, Tomas Wallenius, «Method for estimating wind turbine production losses due to icing», 2013